

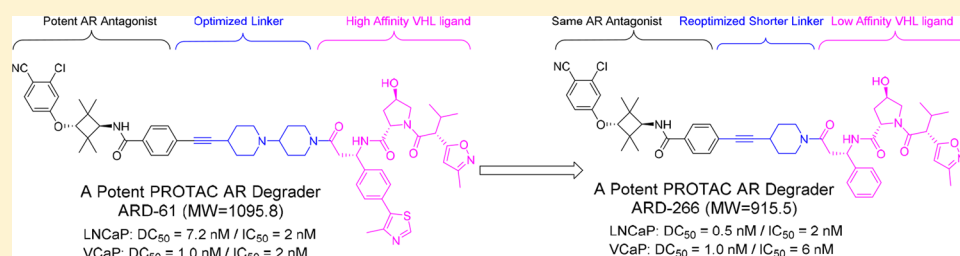
# Discovery of Highly Potent and Efficient PROTAC Degraders of Androgen Receptor (AR) by Employing Weak Binding Affinity VHL E3 Ligase Ligands

Xin Han,<sup>†,+,±</sup> Lijie Zhao,<sup>†,+,⊗,±</sup> Weiguo Xiang,<sup>†,+</sup> Chong Qin,<sup>†,+</sup> Bukeyan Miao,<sup>†,+</sup> Tianfeng Xu,<sup>†,+</sup> Mi Wang,<sup>†,+</sup> Chao-Yie Yang,<sup>†,+</sup> Krishnapriya Chinnaswamy,<sup>#</sup> Jeanne Stuckey,<sup>#</sup> and Shaomeng Wang<sup>\*,†,+,Ⓛ,Ⓢ,Ⓜ</sup>

<sup>†</sup>The Rogel Cancer Center, <sup>+</sup>Department of Internal Medicine, <sup>Ⓛ</sup>Department of Pharmacology, <sup>Ⓢ</sup>Department of Medicinal Chemistry, and <sup>#</sup>Life Sciences Institute, University of Michigan, Ann Arbor, Michigan 48109, United States

<sup>⊗</sup>School of Pharmaceutical Sciences and Institute of Drug Discovery & Development, Zhengzhou University, Zhengzhou 450001, China

## Supporting Information



**ABSTRACT:** Androgen receptor (AR) is a validated therapeutic target for the treatment of metastatic castration-resistant prostate cancer (mCRPC). We report herein our design, synthesis, and biological characterization of highly potent small-molecule proteolysis targeting chimera (PROTAC) AR degraders using a potent AR antagonist and E3 ligase ligands with weak binding affinities to VHL protein. Our study resulted in the discovery of **11** (ARD-266), which effectively induces degradation of AR protein in AR-positive (AR+) LNCaP, VCaP, and 22Rv1 prostate cancer cell lines with DC<sub>50</sub> values of 0.2–1 nM. ARD-266 is capable of reducing the AR protein level by >95% in these AR+ prostate cancer cell lines and effectively reduces AR-regulated gene expression suppression. For the first time, we demonstrated that an E3 ligand with micromolar binding affinity to its E3 ligase complex can be successfully employed for the design of highly potent and efficient PROTAC degraders and this finding may have a significant implication for the field of PROTAC research.

## INTRODUCTION

In the past few years, induced targeted protein degradation based on the proteolysis targeting chimera (PROTAC) concept has gained momentum as a new small-molecule therapeutic strategy.<sup>1–16</sup> One major advantage of this new therapeutic strategy is that, by reducing protein levels, PROTAC small-molecule degraders can achieve more complete target inhibition than traditional small-molecule inhibitors and are predicted to be therapeutically more efficacious.<sup>17–20</sup> Indeed, our recent studies have demonstrated that PROTAC degraders of BET proteins, MDM2 protein, the androgen receptor (AR), and the estrogen receptor (ER) are indeed much more potent and effective against cancer cells than the corresponding inhibitors.<sup>21–26</sup>

A typical PROTAC degrader consists of a ligand, which binds to the target protein of interest, and is tethered by a chemical linker to a second ligand, which binds to and recruits an E3 ligase complex system.<sup>27–33</sup> In the design of a highly potent and effective PROTAC degrader, it has generally been assumed that high-affinity ligands for the target protein and

the E3 ligase complex, together with an appropriate linker, are required for the formation of a productive ternary degradation complex to achieve efficient degradation of the target protein.<sup>34–37</sup> To date, the influence of the ligand affinity to the target protein and the linker on the potency and efficiency of PROTAC degraders have been investigated.<sup>21,26</sup> However, to the best of our knowledge, how the binding affinity of a ligand for an E3 ligase complex affects potency, efficiency, and kinetics of the resulting PROTAC degraders has not been investigated.

We recently reported the discovery of **1** (ARD-61) as a highly potent and efficient PROTAC AR degrader. The structure of ARD-61 includes a potent AR antagonist, a high-affinity ligand for the VHL/cullin2 E3 ligase complex, and an optimized linker.<sup>26</sup> In our present study, we have investigated how the binding affinity of the VHL ligand portion to VHL protein influences the potency and efficiency of the resulting

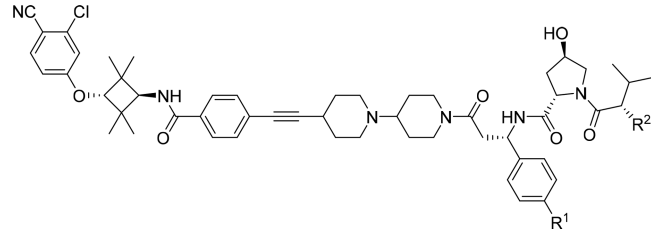
Received: August 22, 2019

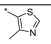
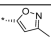
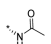
Published: December 5, 2019

Table 1. Binding Affinities of VHL Ligands to VHL Protein, from an FP-Based Binding assay<sup>a</sup>

VHL ligand	VHL-a	VHL-b	VHL-c	VHL-d	VHL-e	VHL-f	VHL-g	VHL-h
IC <sub>50</sub> ± SD (μM)	0.025 ± 0.004	0.21 ± 0.04	1.08 ± 0.07	0.98 ± 0.15	2.52 ± 0.3	10.5 ± 1.6	9.9 ± 0.5	>100
K <sub>i</sub> ± SD (μM)	0.006 ± 0.001	0.058 ± 0.011	0.31 ± 0.02	0.28 ± 0.04	0.72 ± 0.09	3.0 ± 0.5	2.8 ± 0.2	

<sup>a</sup>All of the data are an average of three independent experiments.

Table 2. Investigation of the VHL Ligand Binding Potencies on AR Degradation in PROTAC AR Degraders<sup>a</sup>


Compound	R <sup>1</sup>	R <sup>2</sup>	% AR protein degradation in LNCaP Cells (μM)		
			0.01	0.1	1
1 (ARD-61)			76	>95	>99
2	≡		68	>95	>99
3	CN		81	>95	>99
4	Br		45	76	>95
5	Cl		85	>95	>99
6	F		92	>95	>99
7	H		62	72	>99
8	H		8	11	17

<sup>a</sup>All of the data are an average of three independent experiments with a treatment time of 6 h.

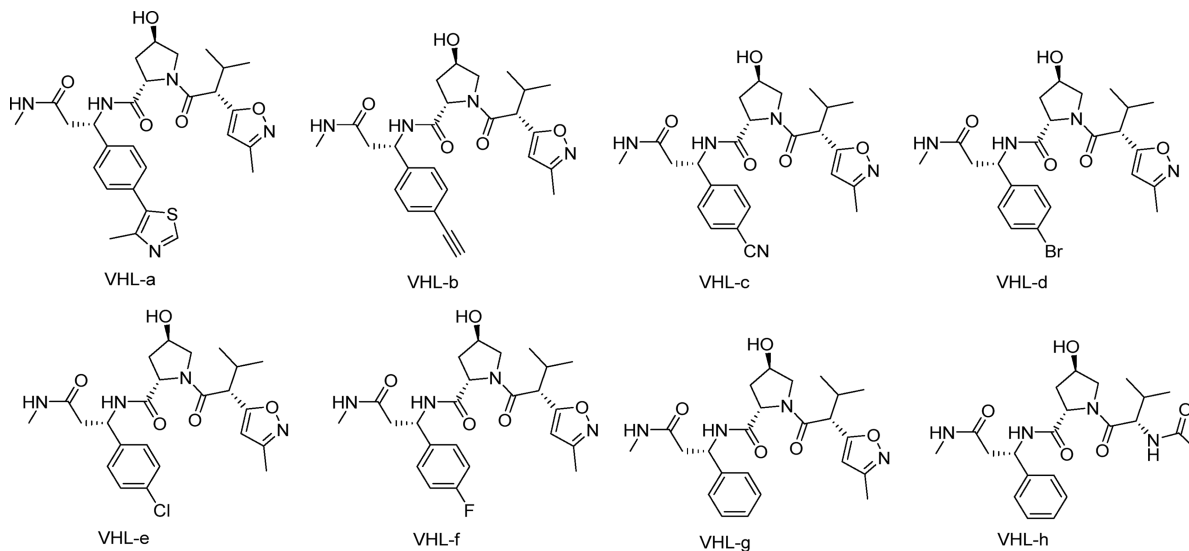


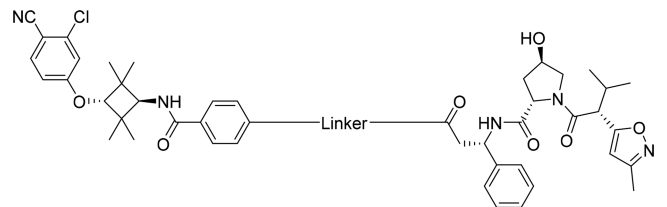
Figure 1. Structures of VHL ligands.

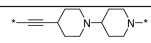
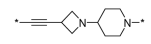
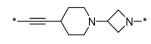
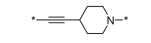
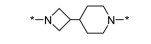
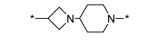
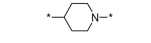
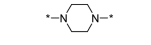
PROTAC degraders. Our study demonstrates that, surprisingly, highly potent and efficient PROTAC degraders can be obtained using VHL ligands with a weak affinity ( $K_i = 2\text{--}3\ \mu\text{M}$ ) to VHL protein.

## RESULTS AND DISCUSSION

**Design and Synthesis of VHL Ligands with a Wide Range of Binding Affinities.** In our previous study, we successfully developed highly potent and efficient AR

degraders based on high-affinity VHL E3 ligase ligands and several classes of AR antagonists.<sup>26</sup> One such highly potent AR degrader is **1** (ARD-61) (Table 2), which achieves DC<sub>50</sub> (concentration needed to degrade 50% of AR protein) values of 1–10 nM in LNCaP and VCaP AR+ prostate cancer cell lines. ARD-61 is also capable of achieving a  $D_{\text{max}}$  (maximal levels of protein degradation) of >95%. In the same study, we found that the linker and AR antagonist portions of the AR degraders have a major effect on the degradation potency.

Table 3. Investigation of the Effect of the Linker on AR Degradation in AR Degraders<sup>a</sup>


Compound	Linker	% AR protein degradation in LNCaP Cells ( $\mu\text{M}$ )		
		0.01	0.1	1
7		62	72	>99
9		6	68	86
10		21	67	68
11 (ARD-266)		90	>95	>99
12		48	>95	>99
13		40	>95	>99
14		38	>95	>99
15		<5	>95	>99

<sup>a</sup>All of the data are an average of three independent experiments with a treatment time of 6 h.

However, the effect of the VHL portion in our previously reported AR degraders on AR degradation has not been investigated. We therefore decided to examine how the VHL ligand portion affects the AR degradation in our designed AR degraders using ARD-61 as the template molecule.

Co-crystal structures for a number of VHL ligands in a complex with VHL protein showed that the 4-methylthiazole group of the ligand VHL-a binds to a hydrophobic pocket in the VHL protein.<sup>9,38–41</sup> Accordingly, we designed and synthesized a number of VHL ligands based on VHL-a (Figure 1) by replacing the 4-methylthiazole group with different groups and tested their binding affinities to VHL protein using our optimized fluorescence polarization (FP)-based binding assay.<sup>26</sup>

Replacement of the 4-methylthiazole group in VHL-a with an ethyne group resulted in VHL-b, which binds to VHL protein with an  $\text{IC}_{50}$  value of 210 nM ( $K_i = 58$  nM) and is 10 times less potent than VHL-a. Replacing the 4-methylthiazole group with a nitrile, Br, Cl, F, and H generated VHL-c, VHL-d, VHL-e, VHL-f, and VHL-g, respectively, which bind to VHL protein with  $K_i$  values of 0.31, 0.28, 0.72, 3.0, and 2.8  $\mu\text{M}$ , respectively. Hence, VHL-c, VHL-d, VHL-e, VHL-f, and VHL-g are 52, 47, 120, 500, and 467 times less potent than VHL-a based on their  $K_i$  values in binding to VHL protein. We next changed the 3-methylisoxazole group in VHL-g with an acetyl group, yielding VHL-h, which shows no appreciable binding to VHL protein up to 100  $\mu\text{M}$ . Hence, our modifications of VHL-a have yielded a series of VHL ligands with a wide range of binding affinities to VHL protein.

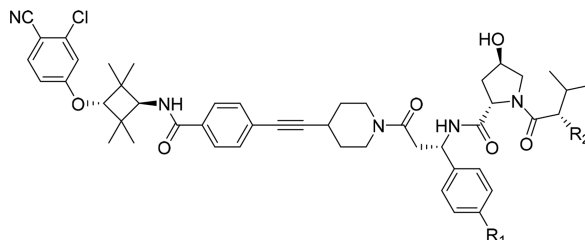
**Design and Synthesis of PROTAC AR Degraders Using VHL Ligands with a Wide Range of Binding Affinities.** We employed 1 (ARD-61) as our template AR degrader and synthesized a series of new PROTAC AR degraders (Table 2) using the VHL ligands shown in Figure 1, which have a wide range of binding affinities to VHL. We tested these putative AR degraders at 10 nM, 100 nM, and 1

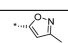
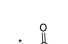
$\mu\text{M}$  for their effect on the levels of AR protein in the AR+ LNCaP prostate cancer cell line, obtaining the data summarized in Table 2.

Compound 8, which consists of a VHL ligand showing no appreciable binding to VHL protein at 100  $\mu\text{M}$ , fails to reduce the levels of AR protein significantly at 10 nM, 100 nM, and 1  $\mu\text{M}$ . Interestingly, all other putative AR degraders, consisting of VHL ligands with a wide range of binding affinities to VHL protein, effectively reduce the levels of AR protein at each of the three concentrations (10 nM, 100 nM, and 1  $\mu\text{M}$ ). Compounds 3, 5, and 6, all of which contain a VHL ligand with much weaker binding affinities to VHL protein than that in ARD-61, are as potent as ARD-61 in reducing the levels of AR proteins. In fact, these three compounds are capable of reducing the AR protein level by >80% at 10 nM, showing their very high potency.

**Further Optimization of the Linker in AR Degraders.** Although compound 7 is not the most potent AR degrader in Table 2, it contains a VHL ligand with a quite weak affinity ( $\text{IC}_{50} = 9.9$   $\mu\text{M}$  and  $K_i = 2.8$   $\mu\text{M}$ ) to VHL protein. Our previous study showed that optimization of the linker length and composition of AR degraders can significantly improve their degradation potency. Accordingly, we performed further modifications of the linker in 7, and the results are summarized in Table 3.

Compounds 9 and 10 were synthesized by replacing the linker consisting of a six-six-membered ring with a four-six-membered ring and a six-four-membered ring linker, respectively. Our Western blotting data showed that both compounds 9 and 10 effectively induce AR degradation in the LNCaP AR+ cell line but are less potent than compound 7. We removed one six-membered ring in the linker of compound 7, yielding compound 11 (ARD-266), which reduces the AR protein by >90% at 10 nM and is more potent than 7. We replaced the ethyne group in the linker of ARD-266 with an azetidine group, affording the isomeric

Table 4. Investigation of the VHL Ligand Portion in ARD-266<sup>a</sup>


Compound	R <sup>1</sup>	R <sup>2</sup>	% AR protein degradation in LNCaP Cells (μM)		
			0.01	0.1	1
<b>11</b> (ARD-266)	H		90	>95	>99
<b>16</b>	4-methylthiazole		56	>95	>99
<b>17</b>	F		62	>95	>99
<b>18</b>	Cl		85	>95	>99
<b>19</b>	Br		31	>95	>99
<b>20</b>	CN		80	>95	>99
<b>21</b>	≡		76	>95	>99
<b>22</b>	H		<5	<5	<5

<sup>a</sup>All of the data are an average of three independent experiments with a treatment time of 6 h.

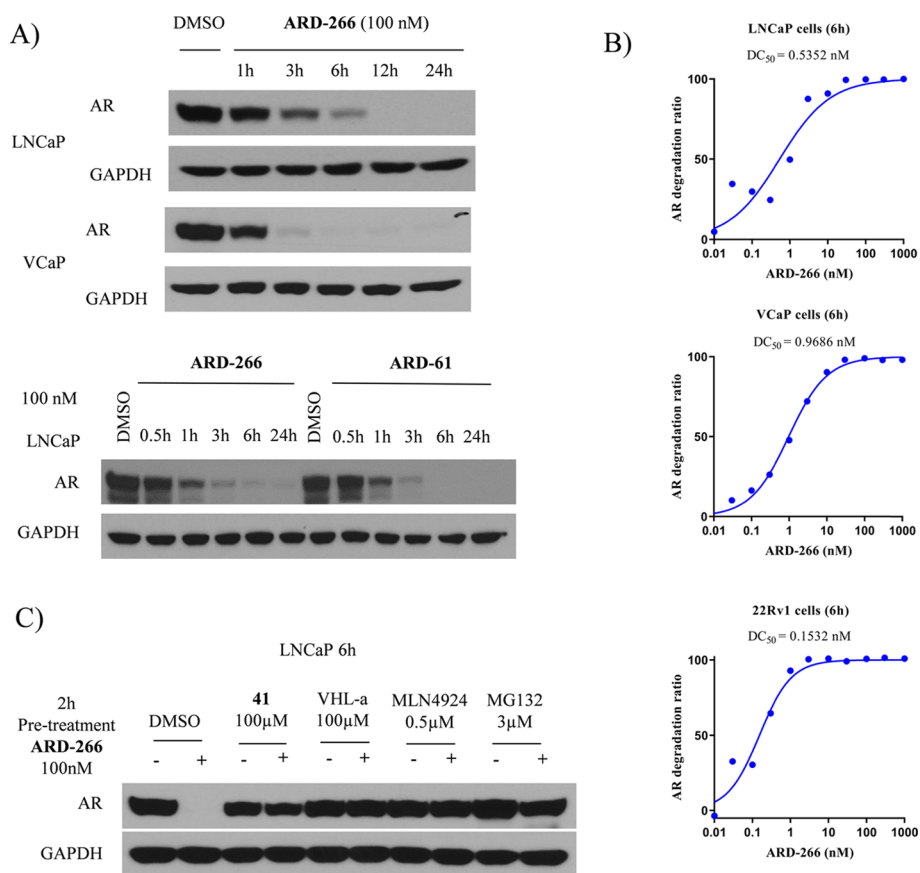


**Figure 2.** Western blotting analysis of AR protein in AR+ prostate cancer cell lines. (A) Immunoblots in LNCaP and VCaP cells treated with AR degraders **11** (ARD-266) and **1** (ARD-61), with GAPDH used as the loading control at different time points; Cells were treated with 100 nM of ARD-266 or of ARD-61 for indicated times. (B) Plots of immunoblots (SI, Figure S2) in LNCaP, VCaP, and 22Rv1 cells treated with AR degrader ARD-266 at different concentrations for 6 hr. (C) Mechanistic investigation of AR degradation induced by ARD-266 in LNCaP cells; cells were pretreated with AR antagonist **41**, VHL-a, MLN4924, and MG132 followed by a 6 h treatment with ARD-266 at 100 nM.

compounds **12** and **13**. While both **12** and **13** are very effective in inducing near-complete AR degradation at 100 nM

and 1 μM, they reduce the levels of AR protein by only 40% at 10 nM and are thus less potent than ARD-266. Removal of

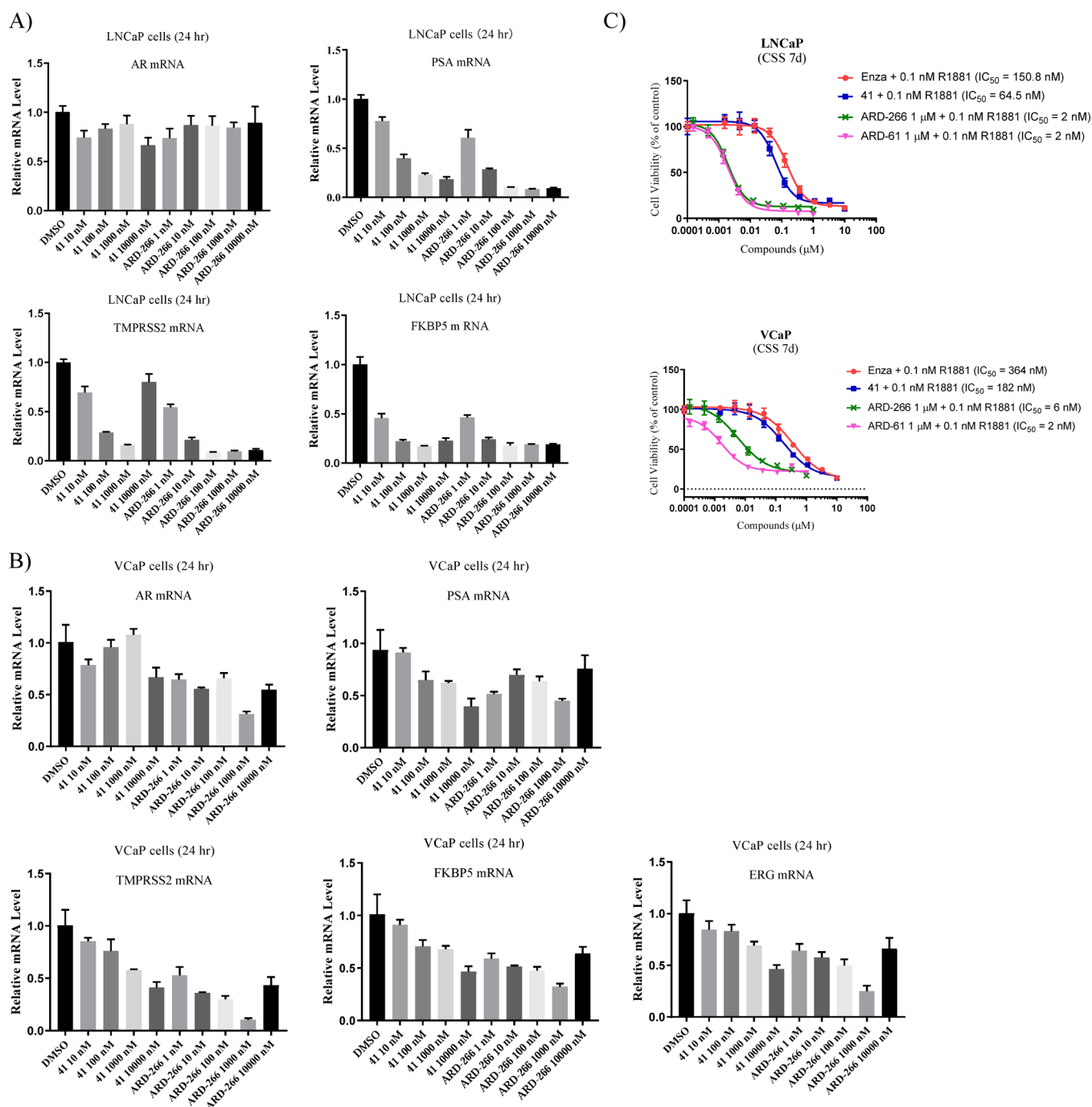


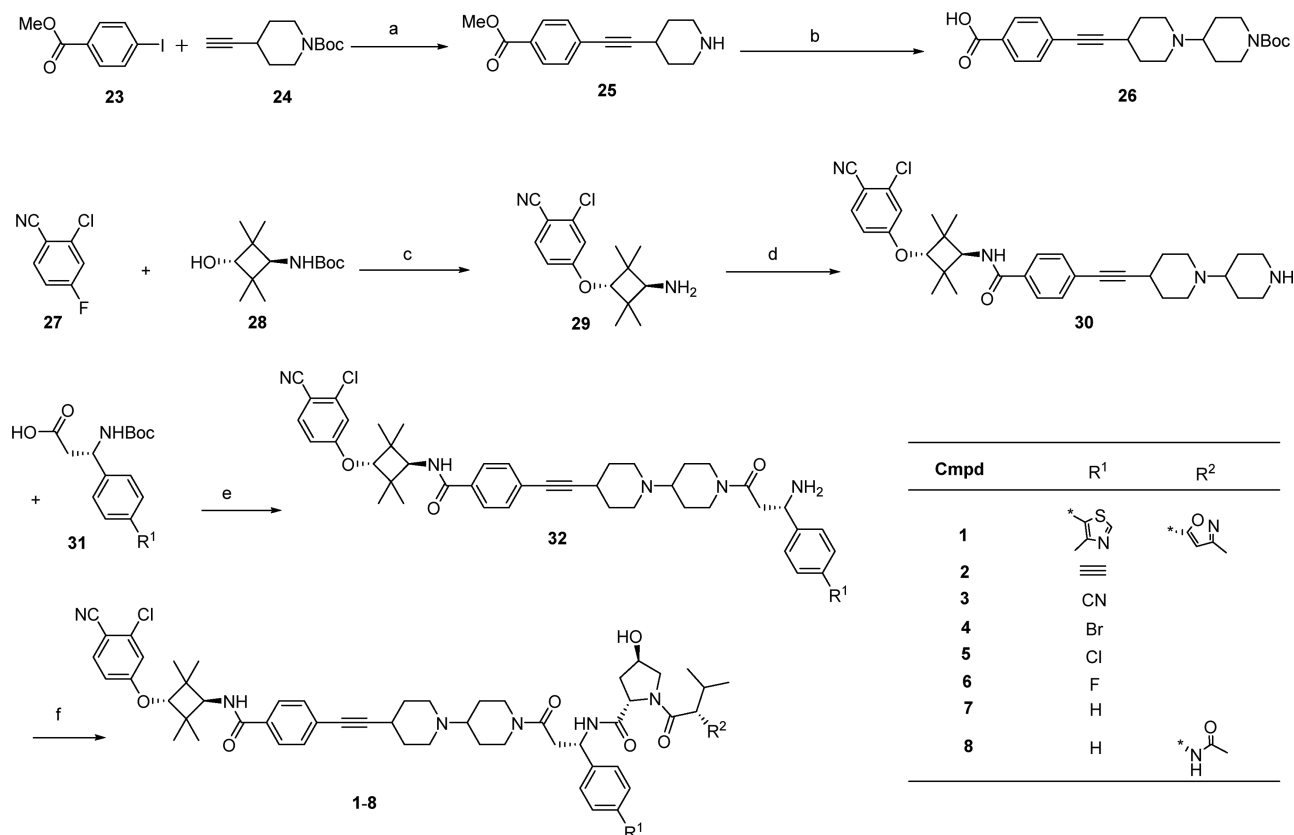
**Figure 3.** (A) Suppression of AR-regulated gene expression in the LNCaP cell line by the AR degrader 11 (ARD-266) and the AR antagonist 41. LNCaP cells were treated for 24 h, and qRT-PCR was performed to determine the mRNA levels for AR and AR-regulated genes. (B) Suppression of AR-regulated gene expression in the VCaP cell line by the AR degrader ARD-266 and the AR antagonist 41. VCaP cells were treated for 24 h, and qRT-PCR was performed to determine the mRNA levels for AR and AR-regulated genes. (C) Cell growth inhibition in LNCaP and VCaP cells treated with AR degrader ARD-266, 1 (ARD-61) and two AR antagonists enzalutamide and 41. LNCaP and VCaP cells were treated with different compounds in a charcoal-stripped medium in the presence of 0.1 nM AR agonist R1881 for 7 days. Cell viability was determined by a WST-8 assay.

the ethyne group in the linker of ARD-266 resulted in **14**, which is still a very potent AR degrader but is less potent than ARD-266. Changing the piperidinyl group in the linker in **14** with a piperazinyl group led to **15**, which is capable of reducing the AR protein by >95% at 100 nM and 1  $\mu\text{M}$  but is less effective than **14** at 10 nM.

**Examination of the VHL Ligand Portion in ARD-266.** Compound **11** (ARD-266) is a highly potent AR degrader and

is capable of reducing AR protein by >90% even at 10 nM. We performed further modifications of the VHL ligand portion of ARD-266, with the results summarized in Table 4.

We replaced the relatively weak VHL ligand in ARD-266 with the high-affinity VHL ligand used in ARD-61, yielding **16**. While **16** is very potent and effective in reducing the AR protein in the LNCaP cell line, it is less potent than ARD-266 at 10 nM.

Scheme 1. Compounds 1–8<sup>a</sup>

<sup>a</sup>Reaction conditions: (a) CuI, PdCl<sub>2</sub>(PPh<sub>3</sub>)<sub>2</sub>, DMF/TEA, 100 °C; TFA, DCM, room temperature (rt); (b) K<sub>2</sub>CO<sub>3</sub>, KI, CH<sub>3</sub>CN, reflux; NaOH, MeOH/H<sub>2</sub>O, rt; (c) NaH, DMF, rt; TFA, DCM, rt; (d) HATU, DIPEA, DMF, rt; TFA, DCM, rt; (e) HATU, DIPEA, DMF, rt; TFA, DCM, rt; (f) HATU, DIPEA, DMF, rt.

A F, Cl, Br, nitrile, or ethylene group was installed onto the 4-position of the phenyl ring in ARD-266, leading to compounds 17–21, respectively. All these compounds can reduce AR protein by >95% at concentrations of 100 nM and 1 μM. At 10 nM, 18 and 20 are still capable of reducing AR protein by ≥80% but are less effective than ARD-266. Since a number of these AR degraders employ a VHL ligand, which has a greater affinity than that in ARD-266, the data showed that employing a more potent VHL ligand does not necessarily result in more potent AR degraders.

Finally, we synthesized compound 22 using a VHL ligand, which does not have an appreciable binding to VHL protein up to 100 μM. Compound 22 has no effect on the levels of AR protein at concentrations of 10–1000 nM.

**Further Evaluation of ARD-266 in AR-Positive Prostate Cancer Cell Lines.** Our data in the LNCaP cell line demonstrated that ARD-266 is a very potent and effective AR degrader, and next we further evaluated ARD-266 in AR-positive prostate cancer cell lines for its activity and mechanism of action.

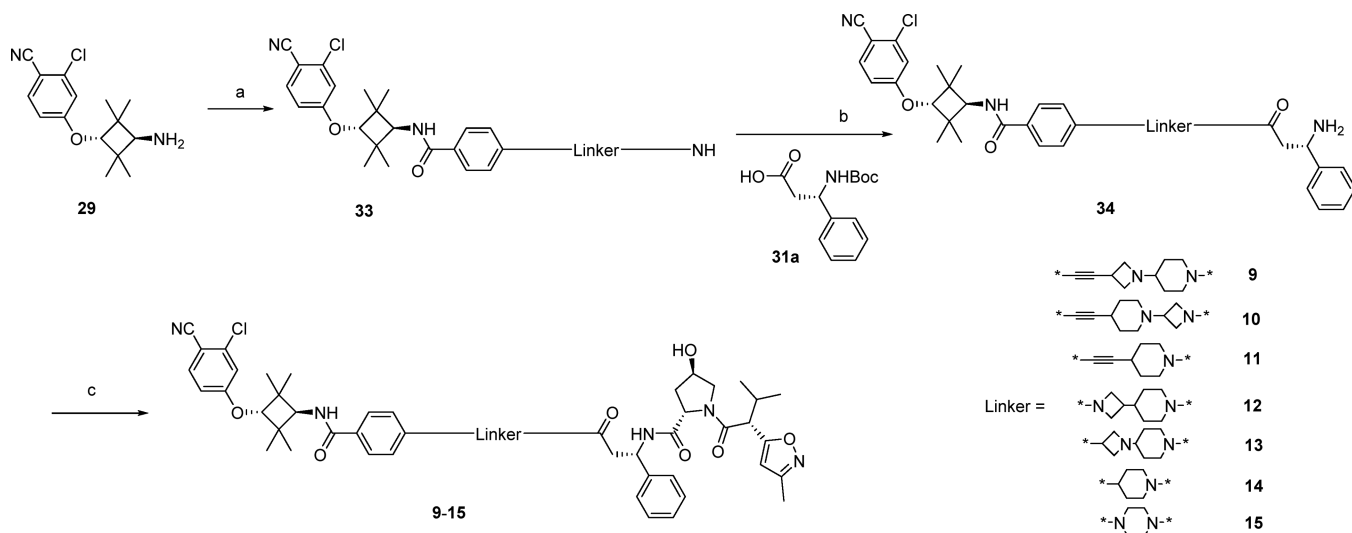
We examined the kinetics of ARD-266 in the induction of AR degradation in LNCaP and VCaP AR+ prostate cancer cell lines, and the results are shown in Figure 2. The data show that ARD-266 effectively reduces the AR protein level within 3 h and achieves near-complete AR elimination with a 6 h treatment in the LNCaP cells. In VCaP cells, ARD-266 reduces the AR protein level by >90% after a 3 h treatment. Our kinetic data thus show that the induction of AR degradation by ARD-266 in these AR+ prostate cancer cell

lines is fairly rapid. In comparison, ARD-266 and ARD-61 degrade AR protein with a very similar kinetics (Figure 2A).

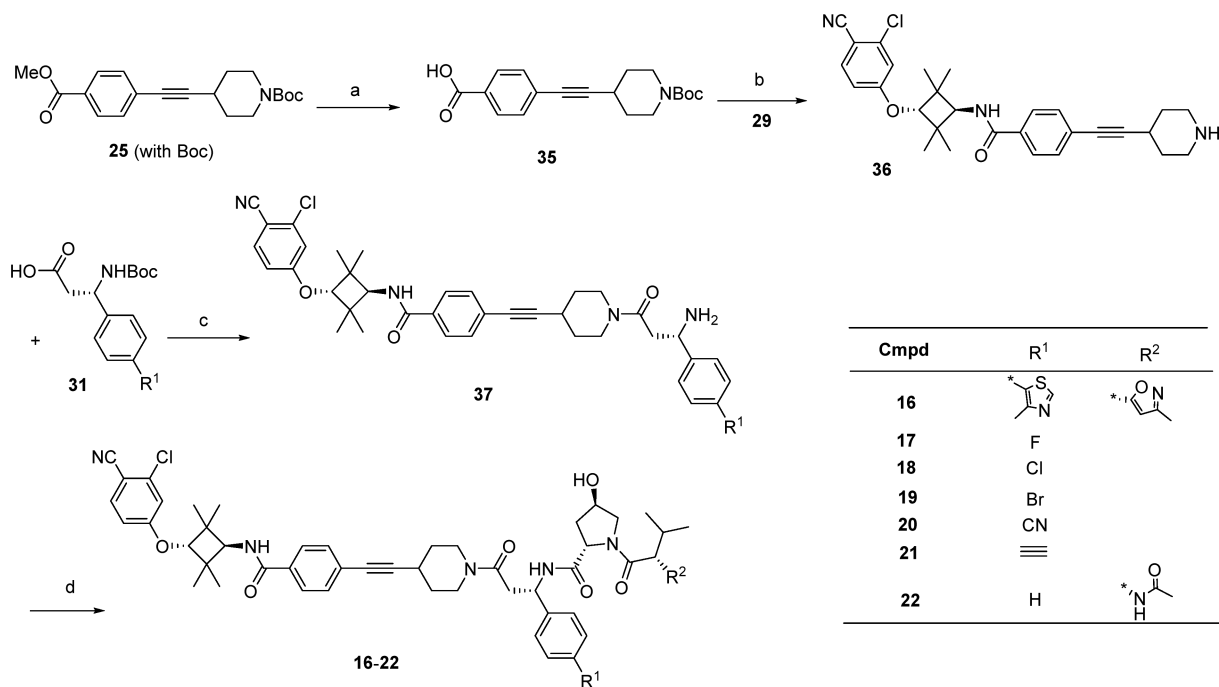
We next tested ARD-266 for its potency in LNCaP, VCaP, and 22Rv1 AR-positive prostate cancer cell lines. Our Western blotting data showed that ARD-266 induces AR degradation in a dose-dependent manner in each of these three cell lines. ARD-266 achieves DC<sub>50</sub> values of 0.5, 1, and 0.2 nM in the LNCaP, VCaP, and 22Rv1 cell lines, respectively. ARD-266 is able to reduce the AR protein level by >95% at 30 nM in both the LNCaP and VCaP cell lines and at 10 nM in the 22Rv1 cell line with a 6 h treatment time (Figure 2B and Supporting Information).

We investigated the mechanism of action of ARD-266 in inducing AR protein degradation in the LNCaP cell line, obtaining the results shown in Figure 2C. Our data showed that AR degradation induced by ARD-266 can be effectively blocked by pretreatment with an AR antagonist (41), a VHL ligand (VHL-a, Figure 1), a NEDD8-activating E1 enzyme inhibitor (MLN4924) and a proteasome inhibitor (MG132) in the LNCaP cell line. These mechanistic data clearly demonstrate that ARD-266 is a bona fide AR degrader.

We next evaluated the ability of ARD-266 to suppress AR-regulated gene expression in the LNCaP and VCaP cell lines, with an AR antagonist (41) included as the control (Figure 3A,B). Our data showed that ARD-266 effectively suppresses the expression of *PSA*, *TMPRSS2*, and *FKBP5* genes in a dose-dependent manner and is capable of reducing the mRNA levels of *PSA*, *TMPRSS2*, and *FKBP5* genes by >50% at 10 nM in the LNCaP cell line. In the VCaP cell line, ARD-266

Scheme 2. Compounds 9–15<sup>a</sup>

<sup>a</sup>Reaction conditions: (a) HATU, DIPEA, DMF, rt; TFA, DCM, rt; (b) HATU, DIPEA, DMF, rt; TFA, DCM, rt; (c) HATU, DIPEA, DMF, rt.

Scheme 3. Compounds 16–22<sup>a</sup>

<sup>a</sup>Reaction conditions: (a) NaOH, MeOH/H<sub>2</sub>O, rt; (b) HATU, DIPEA, DMF, rt; TFA, DCM, rt; (c) HATU, DIPEA, DMF, rt; TFA, DCM, rt; (d) HATU, DIPEA, DMF, rt.

can also suppress the expression of *TMPRSS2* and *FKBP5* genes by 50% at 10 nM and *ERG* gene by 50% at 100 nM. In a direct comparison, ARD-266 is therefore >10–100 times more potent than the AR antagonist 41 in suppressing the AR-regulated gene transcription in both the LNCaP and VCaP cell lines.

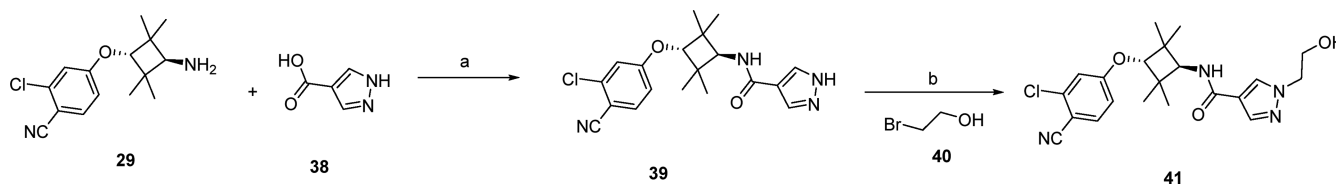
We tested the ability of ARD-266 to inhibit cell growth, with enzalutamide and compound 41 included as AR antagonist controls in the LNCaP and VCaP cell lines, obtaining the data shown in Figure 3C.

Our data showed that ARD-266 potently and effectively inhibits cell growth in the LNCaP cell line and has an IC<sub>50</sub> value of 2 nM. In direct comparison, the AR antagonist 41 has

an IC<sub>50</sub> value of 64.5 nM and is thus >30 times less potent than ARD-266. In the VCaP cell line, ARD-266 and the AR antagonist 41 have IC<sub>50</sub> values of 6 and 182 nM, respectively. Hence, ARD-266 is 30 times more potent than 41 in inhibition of cell growth in the VCaP cell line. In both the LNCaP and VCaP cell lines, enzalutamide is slightly less potent than compound 41 in inhibition of cell growth (Figure 3C).

## CHEMISTRY

The synthesis of compounds 1–8 is shown in Scheme 1. The compound 25 was synthesized from the Sonogashira coupling

Scheme 4. Compound 41<sup>a</sup>

<sup>a</sup>Reaction conditions: (a) HATU, DIPEA, DMF, rt; (b) K<sub>2</sub>CO<sub>3</sub>, KI, CH<sub>3</sub>CN, reflux.

reaction of the compounds 23 and 24. Compound 26 was produced through the hydrolysis and substitution reaction of intermediate 25 with *tert*-butyl 4-bromopiperidine-1-carboxylate. As shown in Scheme 1, the key intermediate 30 was synthesized in two steps. Compounds 32 can be obtained from the amidation of compound 30 with different amino acids (31). Finally, the target compounds were obtained through the amidation of intermediate 32 and different VHL fragments.

Compounds 9–15 were synthesized according to the method shown in Scheme 2. An amidation reaction of compound 29 with different type of linkers gave the key intermediates (33). The intermediates (34) were made by amidation of compounds 32 with (*S*)-3-((*tert*-butoxycarbonyl)amino)-3-phenylpropanoic acid 31a. The target compounds 9–15 were obtained by amidation of 34 with (2*S*,4*R*)-4-hydroxy-1-((*R*)-3-methyl-2-(3-methylisoxazol-5-yl)butanoyl)pyrrolidine-2-carboxylic acid.

The synthesis of compounds 16–22 is shown in Scheme 3. Compound 35 was produced by hydrolysis of the intermediate Boc-protected 25. Compound 36 was made by amidation of compounds 29 and 35. As shown in Scheme 3, the key intermediates 37 were synthesized from the amidation of compound 34 with different amino acids (31). Finally, the target compounds were obtained through amidation of the intermediates 35 and various VHL fragments.

Compound 41 was synthesized according to the reported method.<sup>42</sup> As shown in Scheme 4, the key intermediate 39 was synthesized from the amidation of compound 29 with 34. Then, the target compound 41 was obtained through the substitution reaction of the intermediates 39 and 2-bromoethanol (40).

## CONCLUSIONS

In this study, we designed, synthesized, and evaluated a series of putative PROTAC AR degraders using a potent AR antagonist and VHL E3 ligase ligands with a wide range of binding affinities to VHL protein. The study demonstrated that highly potent and efficient AR degraders can be successfully obtained using VHL ligands with a weak affinity to VHL, exemplified by 1 (ARD-266). Although ARD-266 consists of a VHL ligand with a *K*<sub>i</sub> value of 2.8 μM, it is in fact more potent than a number of analogues consisting of a VHL ligand with much higher affinities to VHL and with the same linker and AR antagonist. ARD-266 effectively reduces the AR protein level at concentrations as low as 1 nM in the LNCaP, VCaP, and 22Rv1 AR-positive prostate cancer cell lines. Furthermore, ARD-266 is capable of reducing the AR protein level by >95% at 30 nM with a 6 h treatment time in the LNCaP and VCaP cells. ARD-266 effectively suppresses AR-regulated gene expression in a dose-dependent manner and is effective at concentrations as low as 10 nM in the LNCaP and

VCaP cell lines. Our mechanistic data clearly show that ARD-266 is a bona fide PROTAC AR degrader. Further optimization of ARD-266 may ultimately yield a new class of therapy for the treatment of castration-resistant prostate cancer. While our previous potent AR degrader ARD-61 has a molecular weight (MW) of 1095.5, ARD-266 has an MW of 915.5. We also obtained potent AR degraders 14 and 15, which have MWs of 890.4 and 891.4, respectively. Hence, using VHL ligands with moderate affinities, the MW of the resulting AR degraders can be reduced, and their physicochemical properties can be improved.

In summary, our present study demonstrates for the first time that highly potent and efficient PROTAC degraders can be successfully obtained using a high-affinity ligand to the target protein of interest and an E3 ligase ligand with a micromolar binding affinity to E3. Our study suggests that even using a low-affinity ligand for an E3 ligase complex, the resulting PROTAC degrader can induce the formation of a productive ternary complex consisting of the target protein of interest, the PROTAC degrader, and the E3 ligase complex in cells, leading to efficient degradation of the target protein. Our study may have an important implication for the design of more druglike PROTAC degraders for the purpose of clinical development. Furthermore, since it has been challenging to discover high-affinity ligands for many E3 ligase complexes, our study may open the door to employ E3 ligands with weak binding affinities to E3 ligases for the successful design of highly potent and efficient PROTAC degraders.

## EXPERIMENTAL SECTION

**Chemistry: General Experiment and Information.** Unless otherwise noted, all purchased reagents were used as received without further purification. <sup>1</sup>H NMR and <sup>13</sup>C NMR spectra were recorded on a Bruker Avance 400 MHz spectrometer. <sup>1</sup>H NMR spectra are reported in parts per million (ppm) downfield from tetramethylsilane (TMS). All <sup>13</sup>C NMR spectra are reported in ppm and obtained with <sup>1</sup>H decoupling. In the reported spectral data, the format (δ) chemical shift (multiplicity, *J* values in Hz, integration) was used with the following abbreviations: s = singlet, d = doublet, t = triplet, q = quartet, and m = multiplet. Mass spectral (MS) analysis was carried out with a Waters UPLC mass spectrometer. The final compounds were all purified by a C18 reversed-phase preparative HPLC column with solvent A (0.1% TFA in H<sub>2</sub>O) and solvent B (0.1% TFA in CH<sub>3</sub>CN) as eluents. The purity of all the final compounds was confirmed to be >95% by UPLC-MS or UPLC.

**General Procedure for the Synthesis of Compound (11, ARD-266).** Compounds 23 (10 mmol) and 24 (1.1 equiv), CuI (0.2 equiv), and PdCl<sub>2</sub>(PPh<sub>3</sub>)<sub>2</sub> (0.1 equiv) in DMF and TEA solvents were placed in a 25 mL round-bottom flask under Ar. The mixture was stirred for 4 h at 100 °C and then H<sub>2</sub>O was added into the resulting complex, and the mixture was extracted with EtOAc three times. The organic layer was again washed with H<sub>2</sub>O before being dried over MgSO<sub>4</sub>, and the solvent was removed under vacuum, leaving the crude product. The pure product Boc-protected 25 was obtained by flash column chromatography (hexane/EtOAc = 4:1).



NaOH (2 equiv) was added to a solution of Boc-protected **25** in MeOH/H<sub>2</sub>O and stirred at rt for 2 h. Then, MeOH was removed under reduced pressure, the pH was adjusted with 2 N HCl, and the mixture was extracted with EtOAc. The solvent was removed to afford the product (**35**), which was used without further purification.

NaH (1.2 equiv) was added at 0 °C to a solution of **28** (10 mmol) in dry DMF. After stirring the mixture at 0 °C for 20 min, **27** was added and the mixture was stirred at rt for 4 h. After UPLC-MS demonstrated the full conversion of starting materials, H<sub>2</sub>O was added and the mixture was extracted three times with EtOAc, the combined organic layers were washed with brine, and then dried over anhydrous Na<sub>2</sub>SO<sub>4</sub>. The solvent was removed on a rotary evaporator. The Boc-protected intermediate was obtained by flash column chromatography. Then, the desired intermediate **29** was obtained by deprotection with TFA in DCM in 88% yield.

DIPEA (5 equiv) and HATU (1.2 equiv) were added to a solution of the compound **29** (1 mmol) and **35** (1.1 equiv) in DMF (2 mL). After 30 min at rt, the mixture was subjected to HPLC purification to afford compound **36** in 88% yield after deprotection in TFA/DCM.

DIPEA (5 equiv) and HATU (1.2 equiv) were added to a solution of compound **36** (0.1 mmol) and (S)-3-((tert-butoxycarbonyl)amino)-3-phenylpropanoic acid **31a** (1.1 equiv) in DMF (2 mL). After 30 min at rt, the mixture was subjected to HPLC purification to afford compound **37a** with 80% yield after deprotection in TFA/DCM.

DIPEA (5 equiv) and HATU (1.2 equiv) were added to a solution of the compound **37a** (0.05 mmol) and (2S,4R)-4-hydroxy-1-((R)-3-methyl-2-(3-methylisoxazol-5-yl)butanoyl)pyrrolidine-2-carboxylic acid (1.1 equiv) in DMF (2 mL). After 30 min at rt, the mixture was subject to HPLC purification to afford compound **11** (ARD-266) with 83% yield.

(2S,4R)-N-((S)-3-(4-((1R,3R)-3-(3-Chloro-4-cyanophenoxy)-2,2,4,4-tetramethylcyclobutyl)carbamoyl)phenyl)ethynyl)piperidin-1-yl)-3-oxo-1-phenylpropyl)-4-hydroxy-1-((R)-3-methyl-2-(3-methylisoxazol-5-yl)butanoyl)pyrrolidine-2-carboxamide (**11**, ARD-266). <sup>1</sup>H NMR (400 MHz, MeOD-*d*<sub>4</sub>) δ 7.81–7.77 (m, 2H), 7.74 (d, *J* = 8.7 Hz, 1H), 7.50 (dd, *J* = 8.5, 2.4 Hz, 2H), 7.41–7.32 (m, 4H), 7.30–7.24 (m, 1H), 7.15 (d, *J* = 2.4 Hz, 1H), 7.00 (dd, *J* = 8.8, 2.4 Hz, 1H), 6.23 (dd, *J* = 4.4, 1.9 Hz, 1H), 5.33 (dt, *J* = 30.1, 7.1 Hz, 1H), 4.58–4.37 (m, 2H), 4.30 (d, *J* = 0.9 Hz, 1H), 4.20–4.15 (m, 1H), 4.01–3.84 (m, 2H), 3.82–3.73 (m, 2H), 3.64–3.55 (m, 1H), 3.26 (t, *J* = 9.8 Hz, 1H), 3.12–2.98 (m, 2H), 2.95–2.86 (m, 1H), 2.48–2.38 (m, 1H), 2.30–2.23 (m, 3H), 2.16 (t, *J* = 10.5 Hz, 1H), 1.99 (ddt, *J* = 12.9, 8.3, 4.3 Hz, 1H), 1.81 (dd, *J* = 36.4, 3.5 Hz, 2H), 1.50 (ddd, *J* = 54.1, 15.5, 8.5 Hz, 3H), 1.31 (s, 6H), 1.25 (s, 6H), 1.07 (dd, *J* = 6.6, 2.0 Hz, 3H), 0.94–0.84 (m, 3H). <sup>13</sup>C NMR (100 MHz, MeOD-*d*<sub>4</sub>) δ 171.73, 169.83, 169.55, 169.18, 162.97, 160.17, 159.29, 141.10, 137.56, 135.34, 133.62, 131.17, 128.25, 127.26, 126.92, 126.50, 116.59, 115.73, 114.31, 104.36, 103.08, 93.72, 84.41, 81.00, 80.84, 69.32, 59.58, 59.03, 55.81, 51.05, 50.18, 44.40, 40.23, 40.07, 39.79, 38.23, 37.44, 31.59, 30.91, 27.35, 27.23, 23.03, 22.29, 20.15, 19.59, 19.02, 9.84. HRMS calculated for C<sub>52</sub>H<sub>60</sub>ClN<sub>6</sub>O<sub>7</sub> [M + H]<sup>+</sup>: 915.4212, found 915.4195. UPLC retention time: 6.6 min, purity >95%. Following the procedures used to prepare compound ARD-266, all other compounds were obtained using the same methods.<sup>26</sup>

(2S,4R)-N-((S)-3-(4-((1R,3R)-3-(3-Chloro-4-cyanophenoxy)-2,2,4,4-tetramethylcyclobutyl)carbamoyl)phenyl)ethynyl)-[1,4'-bipiperidin]-1'-yl)-1-(4-(4-methylthiazol-5-yl)phenyl)-3-oxo-propyl)-4-hydroxy-1-((R)-3-methyl-2-(3-methylisoxazol-5-yl)butanoyl)pyrrolidine-2-carboxamide (**1**). <sup>1</sup>H NMR (400 MHz, MeOD-*d*<sub>4</sub>) δ 9.16 (t, *J* = 5.8 Hz, 1H), 7.81 (t, *J* = 8.8 Hz, 2H), 7.74 (d, *J* = 8.7 Hz, 1H), 7.59 (d, *J* = 7.5 Hz, 1H), 7.52 (dd, *J* = 9.1, 5.7 Hz, 5H), 7.14 (d, *J* = 2.1 Hz, 1H), 7.00 (dd, *J* = 8.7, 2.1 Hz, 1H), 6.33–6.20 (m, 1H), 5.53–5.37 (m, 1H), 4.70 (t, *J* = 12.9 Hz, 1H), 4.46 (t, *J* = 18.4 Hz, 2H), 4.31 (s, 2H), 4.17 (s, 1H), 3.90 (dd, *J* = 10.8, 3.8 Hz, 1H), 3.85–3.75 (m, 1H), 3.67–3.51 (m, 4H), 3.28–3.08 (m, 4H), 3.01–2.88 (m, 1H), 2.67 (dd, *J* = 24.1, 11.9 Hz, 1H), 2.56–2.51 (m, 3H), 2.48–2.32 (m, 2H), 2.27 (d, *J* = 4.2 Hz, 3H), 2.25–2.06 (m, 6H), 1.98 (dd, *J* = 10.1, 5.0 Hz, 3H), 1.77 (dd, *J* = 29.2, 14.2 Hz, 1H), 1.62–1.42 (m, 1H), 1.30 (s, 6H), 1.25 (s, 6H), 1.07 (dd, *J* = 13.4,

6.7 Hz, 3H), 0.91–0.84 (m, 3H). HRMS calculated for C<sub>61</sub>H<sub>72</sub>ClN<sub>8</sub>O<sub>7</sub>S [M + H]<sup>+</sup>: 1095.4933, found 1095.4908. UPLC retention time: 5.4 min, purity >95%.

(2S,4R)-N-((S)-3-(4-((1R,3R)-3-(3-Chloro-4-cyanophenoxy)-2,2,4,4-tetramethylcyclobutyl)carbamoyl)phenyl)ethynyl)-[1,4'-bipiperidin]-1'-yl)-1-(4-ethynylphenyl)-3-oxopropyl)-4-hydroxy-1-((R)-3-methyl-2-(3-methylisoxazol-5-yl)butanoyl)pyrrolidine-2-carboxamide (**2**). <sup>1</sup>H NMR (400 MHz, MeOD-*d*<sub>4</sub>) δ 7.86–7.79 (m, 2H), 7.74 (d, *J* = 8.7 Hz, 1H), 7.65–7.58 (m, 1H), 7.53–7.45 (m, 3H), 7.43–7.32 (m, 2H), 7.15 (s, 1H), 7.00 (d, *J* = 8.6 Hz, 1H), 6.25 (d, *J* = 3.7 Hz, 1H), 5.39 (dd, *J* = 17.1, 10.6 Hz, 1H), 4.68 (d, *J* = 11.2 Hz, 1H), 4.53–4.42 (m, 2H), 4.31 (s, 1H), 4.15 (dd, *J* = 23.3, 8.9 Hz, 2H), 3.92–3.76 (m, 2H), 3.52 (ddd, *J* = 34.0, 24.2, 12.1 Hz, 7H), 3.27–3.22 (m, 1H), 3.17–3.03 (m, 3H), 3.02–2.75 (m, 2H), 2.63 (t, *J* = 12.4 Hz, 1H), 2.38 (d, *J* = 13.4 Hz, 2H), 2.27 (d, *J* = 2.7 Hz, 3H), 2.19 (s, 3H), 2.03 (dd, *J* = 27.5, 15.7 Hz, 4H), 1.70–1.52 (m, 1H), 1.39 (dd, *J* = 5.9, 3.8 Hz, 1H), 1.31 (s, 6H), 1.25 (s, 6H), 1.07 (d, *J* = 5.5 Hz, 3H), 0.88 (dd, *J* = 10.1, 4.2 Hz, 3H). UPLC-MS calculated for C<sub>59</sub>H<sub>68</sub>ClN<sub>7</sub>O<sub>7</sub> [M + H]<sup>+</sup>: 1021.49, found 1021.46. UPLC: 5.5 min, purity >95%.

(2S,4R)-N-((S)-3-(4-((1R,3R)-3-(3-chloro-4-cyanophenoxy)-2,2,4,4-tetramethylcyclobutyl)carbamoyl)phenyl)ethynyl)-[1,4'-bipiperidin]-1'-yl)-1-(4-cyanophenyl)-3-oxopropyl)-4-hydroxy-1-((R)-3-methyl-2-(3-methylisoxazol-5-yl)butanoyl)pyrrolidine-2-carboxamide (**3**). <sup>1</sup>H NMR (400 MHz, MeOD-*d*<sub>4</sub>) δ 7.81 (s, 2H), 7.74 (d, *J* = 8.7 Hz, 3H), 7.59 (d, *J* = 8.0 Hz, 3H), 7.52 (d, *J* = 7.0 Hz, 1H), 7.15 (d, *J* = 2.2 Hz, 1H), 7.00 (dd, *J* = 8.7, 2.2 Hz, 1H), 6.31–6.21 (m, 1H), 5.49–5.42 (m, 1H), 4.67 (s, 1H), 4.47 (d, *J* = 7.6 Hz, 2H), 4.31 (s, 1H), 4.22 (s, 1H), 4.18 (s, 1H), 3.84 (dd, *J* = 23.7, 8.8 Hz, 2H), 3.58 (d, *J* = 19.2 Hz, 5H), 3.16 (dd, *J* = 18.3, 11.7 Hz, 4H), 3.02–2.86 (m, 3H), 2.65 (d, *J* = 12.3 Hz, 1H), 2.36 (d, *J* = 12.7 Hz, 2H), 2.27 (s, 3H), 2.18 (s, 4H), 2.02–1.95 (m, 2H), 1.30 (s, 6H), 1.25 (s, 6H), 1.05 (d, *J* = 6.1 Hz, 3H), 0.87 (d, *J* = 6.5 Hz, 3H). UPLC-MS calculated for C<sub>58</sub>H<sub>67</sub>ClN<sub>8</sub>O<sub>7</sub> [M + H]<sup>+</sup>: 1023.49, found 1023.51. UPLC: 5.0 min, purity >95%.

(2S,4R)-N-((S)-1-(4-Bromophenyl)-3-(4-((1R,3R)-3-(3-chloro-4-cyanophenoxy)-2,2,4,4-tetramethylcyclobutyl)carbamoyl)phenyl)ethynyl)-[1,4'-bipiperidin]-1'-yl)-3-oxopropyl)-4-hydroxy-1-((R)-3-methyl-2-(3-methylisoxazol-5-yl)butanoyl)pyrrolidine-2-carboxamide (**4**). <sup>1</sup>H NMR (400 MHz, MeOD-*d*<sub>4</sub>) δ 7.88–7.80 (m, 2H), 7.73 (d, *J* = 8.8 Hz, 1H), 7.59 (q, *J* = 7.4 Hz, 1H), 7.55–7.46 (m, 3H), 7.36–7.26 (m, 2H), 7.14 (d, *J* = 2.4 Hz, 1H), 6.99 (dd, *J* = 8.8, 2.4 Hz, 1H), 6.30–6.20 (m, 1H), 5.46–5.22 (m, 1H), 4.67 (t, *J* = 12.7 Hz, 1H), 4.55–4.37 (m, 2H), 4.31 (d, *J* = 2.6 Hz, 1H), 4.26–4.10 (m, 2H), 3.94–3.71 (m, 2H), 3.67–3.39 (m, 5H), 3.23 (d, *J* = 7.3 Hz, 3H), 3.09 (dd, *J* = 43.6, 12.1 Hz, 3H), 2.63 (s, 1H), 2.44–2.31 (m, 2H), 2.26 (d, *J* = 3.2 Hz, 3H), 2.20–2.11 (m, 3H), 2.05–1.93 (m, 2H), 1.39 (dd, *J* = 6.6, 3.9 Hz, 1H), 1.31 (d, *J* = 2.2 Hz, 6H), 1.24 (s, 6H), 1.06 (dq, *J* = 13.5, 6.0, 4.7 Hz, 3H), 0.86 (ddd, *J* = 9.6, 6.7, 3.7 Hz, 3H). UPLC-MS calculated for C<sub>57</sub>H<sub>68</sub>BrN<sub>7</sub>O<sub>7</sub> [M + H]<sup>+</sup>: 1076.41, found 1076.42. UPLC: 5.3 min, purity >95%.

(2S,4R)-N-((S)-3-(4-((1R,3R)-3-(3-Chloro-4-cyanophenoxy)-2,2,4,4-tetramethylcyclobutyl)carbamoyl)phenyl)ethynyl)-[1,4'-bipiperidin]-1'-yl)-1-(4-chlorophenyl)-3-oxopropyl)-4-hydroxy-1-((R)-3-methyl-2-(3-methylisoxazol-5-yl)butanoyl)pyrrolidine-2-carboxamide (**5**). <sup>1</sup>H NMR (400 MHz, MeOD-*d*<sub>4</sub>) δ 7.86–7.77 (m, 2H), 7.74 (d, *J* = 8.7 Hz, 1H), 7.60 (t, *J* = 7.4 Hz, 1H), 7.52 (d, *J* = 7.8 Hz, 1H), 7.37 (d, *J* = 7.1 Hz, 4H), 7.15 (s, 1H), 7.00 (d, *J* = 8.7 Hz, 1H), 6.25 (t, *J* = 4.5 Hz, 1H), 5.37 (dt, *J* = 11.0, 6.4 Hz, 1H), 4.88–4.77 (m, 2H), 4.68 (t, *J* = 12.2 Hz, 1H), 4.52–4.39 (m, 2H), 4.31 (s, 1H), 4.18 (s, 2H), 3.92–3.73 (m, 2H), 3.65–3.45 (m, 4H), 3.28–3.09 (m, 3H), 3.07–3.00 (m, 1H), 2.98–2.83 (m, 1H), 2.64 (d, *J* = 9.5 Hz, 1H), 2.37 (d, *J* = 14.0 Hz, 2H), 2.30–2.22 (m, 3H), 2.18 (s, 4H), 2.10–1.90 (m, 3H), 1.67 (d, *J* = 9.3 Hz, 1H), 1.30 (s, 6H), 1.25 (s, 6H), 1.11–1.00 (m, 3H), 0.92–0.80 (m, 3H). UPLC-MS calculated for C<sub>57</sub>H<sub>67</sub>C<sub>12</sub>N<sub>7</sub>O<sub>7</sub> [M + H]<sup>+</sup>: 1032.46, found 1032.42. UPLC: 5.2 min, purity >95%.

(2S,4R)-N-((S)-3-(4-((1R,3R)-3-(3-Chloro-4-cyanophenoxy)-2,2,4,4-tetramethylcyclobutyl)carbamoyl)phenyl)ethynyl)-[1,4'-bipiperidin]-1'-yl)-1-(4-fluorophenyl)-3-oxopropyl)-4-hydroxy-1-((R)-3-methyl-2-(3-methylisoxazol-5-yl)butanoyl)pyrrolidine-2-carboxamide (**6**). <sup>1</sup>H NMR (400 MHz, MeOD-*d*<sub>4</sub>) δ 7.82 (dd, *J* = 13.2, 8.2

H<sub>2</sub>, 2H), 7.74 (d, *J* = 8.6 Hz, 1H), 7.60 (t, *J* = 7.3 Hz, 1H), 7.52 (t, *J* = 4.2 Hz, 1H), 7.48–7.35 (m, 2H), 7.15 (d, *J* = 2.3 Hz, 1H), 7.09 (dq, *J* = 14.0, 8.2, 6.1 Hz, 2H), 7.04–6.96 (m, 1H), 6.31–6.19 (m, 1H), 5.38 (dq, *J* = 24.1, 6.5 Hz, 1H), 4.68 (t, *J* = 14.4 Hz, 1H), 4.53–4.36 (m, 2H), 4.34–4.16 (m, 3H), 3.93–3.74 (m, 2H), 3.65–3.50 (m, 4H), 3.33 (p, *J* = 1.7 Hz, 3H), 3.26–3.09 (m, 3H), 3.06–2.84 (m, 2H), 2.65 (q, *J* = 12.6, 12.1 Hz, 1H), 2.44–2.34 (m, 2H), 2.27 (d, *J* = 5.8 Hz, 3H), 2.15 (t, *J* = 11.3 Hz, 4H), 2.05–1.93 (m, 2H), 1.79–1.64 (m, 1H), 1.52–1.40 (m, 1H), 1.33–1.23 (m, 12H), 1.05 (dt, *J* = 12.6, 6.5 Hz, 3H), 0.86 (ddt, *J* = 10.0, 6.9, 3.3 Hz, 3H). UPLC–MS calculated for C<sub>57</sub>H<sub>68</sub>ClN<sub>7</sub>O<sub>7</sub> [M + H]<sup>+</sup>: 1016.49, found 1016.52. UPLC retention time: 4.6 min, purity >95%.

(2*S*,4*R*)-*N*-((*S*)-3-(4-((1*r*,3*r*)-3-(3-Chloro-4-cyanophenoxy)-2,2,4,4-tetramethylcyclobutyl)carbamoyl)phenyl)ethynyl)-[1,4'-bipiperidin]-1'-yl)-3-oxo-1-phenylpropyl)-4-hydroxy-1-((*R*)-3-methyl-2-(3-methylisoxazol-5-yl)butanoyl)pyrrolidine-2-carboxamide (7). <sup>1</sup>H NMR (400 MHz, MeOD-*d*<sub>4</sub>) δ 7.82 (t, *J* = 10.1 Hz, 2H), 7.74 (d, *J* = 8.7 Hz, 1H), 7.61 (t, *J* = 8.3 Hz, 1H), 7.52 (t, *J* = 6.0 Hz, 1H), 7.42–7.29 (m, 5H), 7.15 (d, *J* = 2.4 Hz, 1H), 7.00 (dd, *J* = 8.8, 2.4 Hz, 1H), 6.24 (dd, *J* = 6.4, 2.7 Hz, 1H), 5.43–5.28 (m, 1H), 4.67 (d, *J* = 14.2 Hz, 1H), 4.47 (d, *J* = 13.6 Hz, 2H), 4.31 (s, 1H), 4.23–4.08 (m, 2H), 3.93–3.75 (m, 2H), 3.64–3.47 (m, 4H), 3.23–3.02 (m, 4H), 2.98–2.77 (m, 2H), 2.64 (d, *J* = 12.8 Hz, 1H), 2.45–2.32 (m, 2H), 2.27 (d, *J* = 5.4 Hz, 3H), 2.21–1.90 (m, 8H), 1.69 (d, *J* = 12.8 Hz, 1H), 1.45 (d, *J* = 2.1 Hz, 1H), 1.31 (s, 6H), 1.25 (s, 6H), 1.07 (q, *J* = 6.4 Hz, 3H), 0.91–0.84 (m, 3H). UPLC–MS calculated for C<sub>57</sub>H<sub>68</sub>ClN<sub>7</sub>O<sub>7</sub> [M + H]<sup>+</sup>: 998.49, found 998.43. UPLC retention time: 6.7 min, purity >95%.

(2*S*,4*R*)-1-(Acetyl-L-valyl)-*N*-((*S*)-3-(4-((1*r*,3*r*)-3-(3-chloro-4-cyanophenoxy)-2,2,4,4-tetramethylcyclobutyl)carbamoyl)phenyl)ethynyl)-[1,4'-bipiperidin]-1'-yl)-3-oxo-1-phenylpropyl)-4-hydroxy-pyrrolidine-2-carboxamide (8). <sup>1</sup>H NMR (400 MHz, MeOD-*d*<sub>4</sub>) δ 7.86–7.78 (m, 2H), 7.74 (d, *J* = 8.7 Hz, 1H), 7.62 (dd, *J* = 8.1, 5.2 Hz, 1H), 7.51 (d, *J* = 8.1 Hz, 1H), 7.42–7.27 (m, 5H), 7.16–7.12 (m, 1H), 7.00 (dt, *J* = 8.7, 1.9 Hz, 1H), 5.33 (q, *J* = 6.2, 5.5 Hz, 1H), 4.65 (d, *J* = 13.4 Hz, 1H), 4.55 (t, *J* = 8.3 Hz, 1H), 4.44 (tt, *J* = 8.4, 4.9 Hz, 2H), 4.31 (d, *J* = 3.3 Hz, 1H), 4.18 (d, *J* = 4.9 Hz, 2H), 3.88 (d, *J* = 11.3 Hz, 1H), 3.77 (dq, *J* = 11.6, 4.1 Hz, 1H), 3.59–3.45 (m, 3H), 3.17–2.92 (m, 5H), 2.60 (q, *J* = 13.7 Hz, 1H), 2.39–2.32 (m, 1H), 2.23–2.06 (m, 6H), 2.04–2.01 (m, 3H), 1.95 (ddd, *J* = 13.2, 8.4, 4.4 Hz, 2H), 1.55 (d, *J* = 11.6 Hz, 1H), 1.45–1.38 (m, 1H), 1.28 (dd, *J* = 24.2, 2.9 Hz, 12H), 1.05–0.95 (m, 6H). UPLC–MS calculated for C<sub>55</sub>H<sub>69</sub>ClN<sub>7</sub>O<sub>7</sub> [M + H]<sup>+</sup>: 974.49, found 974.54. UPLC retention time: 4.3 min, purity >95%.

(2*S*,4*R*)-*N*-((*S*)-3-(4-((1*r*,3*r*)-3-(3-Chloro-4-cyanophenoxy)-2,2,4,4-tetramethylcyclobutyl)carbamoyl)phenyl)ethynyl)azetid-1-yl)piperidin-1-yl)-3-oxo-1-phenylpropyl)-4-hydroxy-1-((*R*)-3-methyl-2-(3-methylisoxazol-5-yl)butanoyl)pyrrolidine-2-carboxamide (9). <sup>1</sup>H NMR (400 MHz, MeOD-*d*<sub>4</sub>) δ 7.83 (dd, *J* = 8.3, 2.6 Hz, 2H), 7.74 (d, *J* = 8.8 Hz, 1H), 7.64–7.58 (m, 2H), 7.39–7.27 (m, 5H), 7.15 (d, *J* = 2.4 Hz, 1H), 7.00 (dd, *J* = 8.8, 2.4 Hz, 1H), 6.37–6.21 (m, 1H), 5.62–5.13 (m, 1H), 4.74 (s, 1H), 4.57 (d, *J* = 9.1 Hz, 2H), 4.54–4.38 (m, 5H), 4.31 (s, 1H), 4.18 (s, 1H), 3.97–3.80 (m, 2H), 3.72–3.53 (m, 2H), 3.30–2.99 (m, 4H), 2.69–2.61 (m, 1H), 2.46–2.37 (m, 1H), 2.32–2.24 (m, 3H), 2.15 (s, 3H), 1.97–1.85 (m, 1H), 1.50–1.37 (m, 1H), 1.31 (d, *J* = 1.3 Hz, 6H), 1.25 (s, 6H), 1.10–1.05 (m, 3H), 0.91–0.86 (m, 3H). UPLC–MS calculated for C<sub>55</sub>H<sub>65</sub>ClN<sub>7</sub>O<sub>7</sub> [M + H]<sup>+</sup>: 970.46, found 970.44. UPLC retention time: 5.2 min, purity >95%.

(2*S*,4*R*)-*N*-((*S*)-3-(4-((1*r*,3*r*)-3-(3-Chloro-4-cyanophenoxy)-2,2,4,4-tetramethylcyclobutyl)carbamoyl)phenyl)ethynyl)piperidin-1-yl)azetid-1-yl)-3-oxo-1-phenylpropyl)-4-hydroxy-1-((*R*)-3-methyl-2-(3-methylisoxazol-5-yl)butanoyl)pyrrolidine-2-carboxamide (10). <sup>1</sup>H NMR (400 MHz, MeOD-*d*<sub>4</sub>) δ 7.81 (d, *J* = 8.0 Hz, 2H), 7.73 (dd, *J* = 8.7, 3.1 Hz, 1H), 7.56 (t, *J* = 7.9 Hz, 2H), 7.37 (dt, *J* = 8.5, 3.1 Hz, 4H), 7.30 (dt, *J* = 7.7, 3.7 Hz, 1H), 7.14 (d, *J* = 2.7 Hz, 1H), 7.00 (dd, *J* = 8.7, 2.8 Hz, 1H), 6.37–6.20 (m, 1H), 5.51–5.38 (m, 1H), 4.77–4.62 (m, 1H), 4.58–4.36 (m, 4H), 4.24 (d, *J* = 50.6 Hz, 4H), 3.96–3.79 (m, 2H), 3.72–3.54 (m, 2H), 2.93–2.83 (m, 1H), 2.64 (td, *J* = 14.7, 13.3, 8.2 Hz, 1H), 2.51–2.30 (m, 3H), 2.27 (d, *J* = 14.1 Hz, 3H), 2.06 (ddd, *J* = 57.8, 12.4, 6.7 Hz, 4H), 1.52–

1.36 (m, 1H), 1.32–1.22 (m, 12H), 1.10 (dd, *J* = 13.1, 6.1 Hz, 3H), 0.94–0.84 (m, 3H). UPLC–MS calculated for C<sub>53</sub>H<sub>65</sub>ClN<sub>7</sub>O<sub>7</sub> [M + H]<sup>+</sup>: 970.46, found 970.48. UPLC retention time: 5.0 min, purity >95%.

(2*S*,4*R*)-*N*-((*S*)-3-(4-((1*r*,3*r*)-3-(3-Chloro-4-cyanophenoxy)-2,2,4,4-tetramethylcyclobutyl)carbamoyl)phenyl)azetid-1-yl)piperidin-1-yl)-3-oxo-1-phenylpropyl)-4-hydroxy-1-((*R*)-3-methyl-2-(3-methylisoxazol-5-yl)butanoyl)pyrrolidine-2-carboxamide (12). <sup>1</sup>H NMR (400 MHz, MeOD-*d*<sub>4</sub>) δ 7.80–7.66 (m, 3H), 7.42–7.25 (m, 5H), 7.12 (q, *J* = 2.1 Hz, 1H), 6.97 (dq, *J* = 9.0, 2.1 Hz, 1H), 6.62–6.40 (m, 2H), 6.22 (d, *J* = 1.8 Hz, 1H), 5.41–5.28 (m, 1H), 4.56–4.37 (m, 3H), 4.28 (d, *J* = 1.9 Hz, 1H), 4.15 (s, 1H), 4.00 (tt, *J* = 9.9, 5.4 Hz, 3H), 3.88 (dt, *J* = 11.3, 5.5 Hz, 1H), 3.79 (dd, *J* = 9.6, 7.2 Hz, 1H), 3.75–3.48 (m, 4H), 3.02 (tdt, *J* = 34.9, 15.2, 8.3 Hz, 3H), 2.45 (ddt, *J* = 37.0, 28.9, 10.9 Hz, 4H), 2.25 (d, *J* = 2.0 Hz, 3H), 2.15 (q, *J* = 7.0 Hz, 1H), 1.99 (ttd, *J* = 12.9, 8.9, 8.4, 3.6 Hz, 1H), 1.67 (dd, *J* = 20.2, 11.6 Hz, 3H), 1.29 (s, 6H), 1.22 (d, *J* = 1.9 Hz, 6H), 1.11–1.04 (m, 3H), 0.87 (d, *J* = 6.8 Hz, 3H). UPLC–MS calculated for C<sub>53</sub>H<sub>65</sub>ClN<sub>7</sub>O<sub>7</sub> [M + H]<sup>+</sup>: 946.46, found 946.48. UPLC retention time: 6.4 min, purity >95%.

(2*S*,4*R*)-*N*-((*S*)-3-(4-((1*r*,3*r*)-3-(3-Chloro-4-cyanophenoxy)-2,2,4,4-tetramethylcyclobutyl)carbamoyl)phenyl)azetid-1-yl)piperidin-1-yl)-3-oxo-1-phenylpropyl)-4-hydroxy-1-((*R*)-3-methyl-2-(3-methylisoxazol-5-yl)butanoyl)pyrrolidine-2-carboxamide (13). <sup>1</sup>H NMR (400 MHz, MeOD-*d*<sub>4</sub>) δ 7.91 (dd, *J* = 8.2, 4.6 Hz, 2H), 7.74 (d, *J* = 8.7 Hz, 1H), 7.62–7.55 (m, 2H), 7.37 (tdd, *J* = 10.3, 7.0, 2.5 Hz, 5H), 7.29 (t, *J* = 6.4 Hz, 1H), 7.01 (dd, *J* = 8.7, 2.4 Hz, 1H), 6.38–6.21 (m, 1H), 5.57–5.29 (m, 1H), 4.75–4.37 (m, 9H), 4.32 (s, 1H), 4.19 (s, 1H), 4.02–3.55 (m, 5H), 3.28–3.19 (m, 1H), 3.17–3.03 (m, 1H), 2.95 (d, *J* = 53.3 Hz, 1H), 2.67 (td, *J* = 9.5, 8.3, 4.8 Hz, 1H), 2.45 (dt, *J* = 10.4, 6.5 Hz, 1H), 2.29 (d, *J* = 12.4 Hz, 3H), 2.19 (dd, *J* = 19.7, 10.1 Hz, 4H), 1.98–1.81 (m, 1H), 1.51–1.37 (m, 1H), 1.31 (d, *J* = 2.1 Hz, 6H), 1.25 (s, 6H), 1.13–1.06 (m, 3H), 0.89 (t, *J* = 7.4 Hz, 3H). UPLC–MS calculated for C<sub>53</sub>H<sub>65</sub>ClN<sub>7</sub>O<sub>7</sub> [M + H]<sup>+</sup>: 946.46, found 946.49. UPLC retention time: 5.4 min, purity >95%.

(2*S*,4*R*)-*N*-((*S*)-3-(4-((1*r*,3*S*)-3-(3-Chloro-4-cyanophenoxy)-2,2,4,4-tetramethylcyclobutyl)carbamoyl)phenyl)piperidin-1-yl)-3-oxo-1-phenylpropyl)-4-hydroxy-1-((*R*)-3-methyl-2-(3-methylisoxazol-5-yl)butanoyl)pyrrolidine-2-carboxamide (14). <sup>1</sup>H NMR (400 MHz, DMSO-*d*<sub>6</sub>) δ 7.91 (d, *J* = 8.7 Hz, 1H), 7.78 (d, *J* = 7.8 Hz, 2H), 7.33 (t, *J* = 4.9 Hz, 5H), 7.27–7.18 (m, 3H), 7.01 (dd, *J* = 8.8, 2.4 Hz, 1H), 6.20 (dd, *J* = 17.7, 3.0 Hz, 1H), 5.22 (tt, *J* = 10.4, 8.4, 3.7 Hz, 1H), 4.53 (d, *J* = 12.7 Hz, 1H), 4.42–4.20 (m, 3H), 4.06 (d, *J* = 3.5 Hz, 1H), 3.94 (t, *J* = 16.1 Hz, 1H), 3.76 (dd, *J* = 9.7, 4.2 Hz, 1H), 3.58 (dd, *J* = 11.2, 8.0 Hz, 1H), 3.12–2.74 (m, 4H), 2.62–2.52 (m, 1H), 2.33–2.22 (m, 1H), 2.20 (t, *J* = 4.9 Hz, 3H), 2.02–1.93 (m, 1H), 1.83–1.60 (m, 3H), 1.51–1.36 (m, 1H), 1.19 (d, *J* = 36.7 Hz, 12H), 0.98 (dd, *J* = 6.6, 2.3 Hz, 3H), 0.79 (dd, *J* = 14.2, 6.7 Hz, 3H). UPLC–MS calculated for C<sub>50</sub>H<sub>60</sub>ClN<sub>6</sub>O<sub>7</sub> [M + H]<sup>+</sup>: 891.42, found 891.40. UPLC retention time: 5.2 min, purity >95%.

(2*S*,4*R*)-*N*-((*S*)-3-(4-((1*r*,3*S*)-3-(3-Chloro-4-cyanophenoxy)-2,2,4,4-tetramethylcyclobutyl)carbamoyl)phenyl)piperazin-1-yl)-3-oxo-1-phenylpropyl)-4-hydroxy-1-((*R*)-3-methyl-2-(3-methylisoxazol-5-yl)butanoyl)pyrrolidine-2-carboxamide (15). <sup>1</sup>H NMR (400 MHz, MeOD-*d*<sub>4</sub>) δ 7.81–7.76 (m, 2H), 7.72 (d, *J* = 8.8 Hz, 1H), 7.42–7.31 (m, 4H), 7.28–7.22 (m, 1H), 7.13 (d, *J* = 2.4 Hz, 1H), 7.03–6.95 (m, 3H), 6.19 (s, 1H), 5.44–5.30 (m, 1H), 4.52–4.43 (m, 2H), 4.30 (d, *J* = 0.9 Hz, 1H), 4.16 (d, *J* = 0.9 Hz, 1H), 3.87 (dd, *J* = 10.8, 4.3 Hz, 1H), 3.79–3.53 (m, 6H), 3.31–3.15 (m, 3H), 3.14–2.98 (m, 3H), 2.38 (dtd, *J* = 14.2, 8.5, 7.6, 3.1 Hz, 1H), 2.24 (d, *J* = 3.1 Hz, 3H), 2.16 (dddd, *J* = 13.2, 7.7, 3.0, 1.4 Hz, 1H), 2.07–1.93 (m, 1H), 1.26 (d, *J* = 26.0 Hz, 12H), 1.06 (dd, *J* = 11.7, 6.6 Hz, 3H), 0.88 (dd, *J* = 25.7, 6.7 Hz, 3H). UPLC–MS calculated for C<sub>49</sub>H<sub>59</sub>ClN<sub>7</sub>O<sub>7</sub> [M + H]<sup>+</sup>: 892.42, found 892.43. UPLC retention time: 5.0 min, purity >95%.

(2*S*,4*R*)-*N*-((*S*)-3-(4-((1*r*,3*r*)-3-(3-Chloro-4-cyanophenoxy)-2,2,4,4-tetramethylcyclobutyl)carbamoyl)phenyl)ethynyl)piperidin-1-yl)-1-(4-(4-methylthiazol-5-yl)phenyl)-3-oxopropyl)-4-hydroxy-1-((*R*)-3-methyl-2-(3-methylisoxazol-5-yl)butanoyl)pyrrolidine-2-carboxamide (16). <sup>1</sup>H NMR (400 MHz, MeOD-*d*<sub>4</sub>) δ 9.19–9.09 (m, 1H), 7.89–7.70 (m, 4H), 7.53 (s, 3H), 7.46–7.36 (m, 2H), 7.14 (d,

$J = 2.3$  Hz, 1H), 7.00 (dd,  $J = 8.8, 2.3$  Hz, 1H), 6.35–6.19 (m, 1H), 5.46–5.34 (m, 1H), 4.57–4.40 (m, 2H), 4.31 (s, 1H), 4.18 (s, 1H), 4.10–3.98 (m, 1H), 3.89 (td,  $J = 10.5, 4.1$  Hz, 1H), 3.81 (t,  $J = 9.4$  Hz, 2H), 3.63 (t,  $J = 9.4$  Hz, 1H), 3.29–2.81 (m, 5H), 2.52 (d,  $J = 4.8$  Hz, 3H), 2.47–2.39 (m, 1H), 2.26 (dd,  $J = 6.7, 3.0$  Hz, 3H), 2.18 (dd,  $J = 12.1, 6.2$  Hz, 1H), 2.01 (dddt,  $J = 17.6, 13.2, 8.6, 3.6$  Hz, 1H), 1.85 (s, 2H), 1.60–1.38 (m, 2H), 1.31 (s, 6H), 1.25 (s, 6H), 1.09 (t,  $J = 6.1$  Hz, 3H), 0.89 (td,  $J = 7.2, 6.6, 3.1$  Hz, 3H). HRMS calculated for  $C_{56}H_{63}ClN_6O_7S$  [ $M + H$ ]<sup>+</sup>: 1012.4198, found 1012.4173. UPLC retention time: 6.2 min, purity >95%.

(2*S,4R*)-*N*-((*S*)-3-(4-(((1*r,3r*)-3-(3-Chloro-4-cyanophenoxy)-2,2,4,4-tetramethylcyclobutyl)carbamoyl)phenyl)ethynyl)piperidin-1-yl)-1-(4-fluorophenyl)-3-oxopropyl-4-hydroxy-1-((*R*)-3-methyl-2-(3-methylisoxazol-5-yl)butanoyl)pyrrolidine-2-carboxamide (17). <sup>1</sup>H NMR (400 MHz, MeOD-*d*<sub>4</sub>)  $\delta$  7.79 (dd,  $J = 8.4, 3.3$  Hz, 2H), 7.75–7.71 (m, 1H), 7.49 (dd,  $J = 8.5, 3.4$  Hz, 2H), 7.41 (dd,  $J = 9.2, 5.2$  Hz, 2H), 7.15–7.06 (m, 3H), 6.99 (dt,  $J = 8.7, 3.0$  Hz, 1H), 6.23 (d,  $J = 4.4$  Hz, 1H), 5.35 (d,  $J = 6.3$  Hz, 1H), 4.53–4.42 (m, 2H), 4.30 (d,  $J = 3.8$  Hz, 1H), 4.17 (d,  $J = 3.5$  Hz, 1H), 3.93–3.75 (m, 4H), 3.60 (d,  $J = 10.1$  Hz, 1H), 3.39 (s, 1H), 3.25 (t,  $J = 7.0$  Hz, 1H), 3.13–2.87 (m, 4H), 2.45–2.36 (m, 1H), 2.26 (t,  $J = 4.4$  Hz, 3H), 2.18–2.12 (m, 1H), 1.99 (dq,  $J = 8.5, 4.3$  Hz, 1H), 1.86 (s, 2H), 1.58 (s, 2H), 1.30 (d,  $J = 3.8$  Hz, 6H), 1.24 (t,  $J = 3.0$  Hz, 6H), 1.07 (d,  $J = 5.7$  Hz, 3H), 0.87 (d,  $J = 6.0$  Hz, 3H). UPLC–MS calculated for  $C_{52}H_{59}ClFN_6O_7$  [ $M + H$ ]<sup>+</sup>: 933.41, found 933.42. UPLC retention time: 6.7 min, purity >95%.

(2*S,4R*)-*N*-((*S*)-3-(4-(((1*r,3r*)-3-(3-Chloro-4-cyanophenoxy)-2,2,4,4-tetramethylcyclobutyl)carbamoyl)phenyl)ethynyl)piperidin-1-yl)-1-(4-chlorophenyl)-3-oxopropyl-4-hydroxy-1-((*R*)-3-methyl-2-(3-methylisoxazol-5-yl)butanoyl)pyrrolidine-2-carboxamide (18). <sup>1</sup>H NMR (400 MHz, MeOD-*d*<sub>4</sub>)  $\delta$  7.79 (d,  $J = 7.9$  Hz, 2H), 7.72 (dd,  $J = 7.7, 3.2$  Hz, 3H), 7.58 (d,  $J = 8.2$  Hz, 2H), 7.51 (dt,  $J = 8.2, 4.0$  Hz, 2H), 7.13 (d,  $J = 2.3$  Hz, 1H), 6.98 (dd,  $J = 8.7, 2.3$  Hz, 1H), 6.25 (dd,  $J = 10.2, 3.1$  Hz, 1H), 5.46–5.33 (m, 1H), 4.49 (dd,  $J = 15.9, 7.5$  Hz, 2H), 4.29 (s, 1H), 4.17 (s, 1H), 4.00–3.84 (m, 2H), 3.84–3.73 (m, 2H), 3.61 (d,  $J = 10.7$  Hz, 1H), 3.39 (dd,  $J = 8.3, 4.9$  Hz, 1H), 3.30–3.18 (m, 1H), 3.08 (dtt,  $J = 27.8, 15.5, 6.7$  Hz, 2H), 2.93 (s, 1H), 2.42 (tt,  $J = 15.5, 7.4$  Hz, 1H), 2.26 (d,  $J = 2.9$  Hz, 3H), 2.22–2.12 (m, 1H), 1.98 (dq,  $J = 13.1, 4.5$  Hz, 1H), 1.93–1.80 (m, 2H), 1.66–1.46 (m, 2H), 1.30 (s, 6H), 1.24 (s, 6H), 1.07 (d,  $J = 6.1$  Hz, 3H), 0.93–0.83 (m, 3H). HRMS calculated for  $C_{52}H_{59}Cl_2N_6O_7$  [ $M + H$ ]<sup>+</sup>: 949.3822, found 949.3795. UPLC retention time: 6.5 min, purity >95%.

(2*S,4R*)-*N*-((*S*)-1-(4-Bromophenyl)-3-(4-(((1*r,3r*)-3-(3-chloro-4-cyanophenoxy)-2,2,4,4-tetramethylcyclobutyl)carbamoyl)phenyl)ethynyl)piperidin-1-yl)-3-oxopropyl-4-hydroxy-1-((*R*)-3-methyl-2-(3-methylisoxazol-5-yl)butanoyl)pyrrolidine-2-carboxamide (19). <sup>1</sup>H NMR (400 MHz, MeOD-*d*<sub>4</sub>)  $\delta$  7.79 (d,  $J = 8.0$  Hz, 2H), 7.73 (dd,  $J = 8.7, 2.0$  Hz, 1H), 7.54–7.48 (m, 4H), 7.35–7.28 (m, 2H), 7.13 (d,  $J = 2.2$  Hz, 1H), 6.99 (dt,  $J = 8.9, 2.3$  Hz, 1H), 6.23 (d,  $J = 3.7$  Hz, 1H), 5.37–5.24 (m, 1H), 4.53–4.40 (m, 2H), 4.30 (d,  $J = 1.9$  Hz, 1H), 4.17 (s, 1H), 3.99–3.75 (m, 4H), 3.59 (d,  $J = 10.2$  Hz, 1H), 3.44–3.35 (m, 1H), 3.31–3.20 (m, 1H), 3.09–2.87 (m, 3H), 2.41 (dq,  $J = 20.6, 7.3$  Hz, 1H), 2.28–2.21 (m, 3H), 2.15 (t,  $J = 10.9$  Hz, 1H), 1.98 (ddd,  $J = 13.6, 8.9, 4.7$  Hz, 1H), 1.87 (d,  $J = 13.5$  Hz, 2H), 1.67–1.44 (m, 2H), 1.30 (s, 6H), 1.24 (d,  $J = 1.7$  Hz, 6H), 1.06 (d,  $J = 6.5$  Hz, 3H), 0.88 (dd,  $J = 8.4, 6.3$  Hz, 3H). UPLC–MS calculated for  $C_{52}H_{59}BrClN_6O_7$  [ $M + H$ ]<sup>+</sup>: 993.33, found 993.31. UPLC retention time: 6.6 min, purity >95%.

(2*S,4R*)-*N*-((*S*)-3-(4-(((1*r,3r*)-3-(3-Chloro-4-cyanophenoxy)-2,2,4,4-tetramethylcyclobutyl)carbamoyl)phenyl)ethynyl)piperidin-1-yl)-1-(4-cyanophenyl)-3-oxopropyl-4-hydroxy-1-((*R*)-3-methyl-2-(3-methylisoxazol-5-yl)butanoyl)pyrrolidine-2-carboxamide (20). <sup>1</sup>H NMR (400 MHz, MeOD-*d*<sub>4</sub>)  $\delta$  7.79 (d,  $J = 8.2$  Hz, 2H), 7.73 (d,  $J = 8.7$  Hz, 1H), 7.50 (dd,  $J = 8.4, 2.4$  Hz, 2H), 7.40–7.33 (m, 4H), 7.13 (d,  $J = 2.4$  Hz, 1H), 6.98 (dd,  $J = 8.8, 2.4$  Hz, 1H), 6.23 (d,  $J = 4.2$  Hz, 1H), 5.39–5.29 (m, 1H), 4.55–4.42 (m, 2H), 4.29 (s, 1H), 4.17 (s, 1H), 4.01–3.86 (m, 2H), 3.83–3.74 (m, 2H), 3.60 (d,  $J = 10.9$  Hz, 1H), 3.43–3.35 (m, 1H), 3.30–3.18 (m, 1H), 3.13–2.97 (m, 2H), 2.90 (dt,  $J = 11.0, 5.6$  Hz, 1H), 2.48–2.36 (m, 1H), 2.26 (d,  $J = 4.1$  Hz, 3H), 2.20–2.11 (m, 1H), 1.97 (ddt,  $J = 13.2, 9.2,$

4.7 Hz, 1H), 1.86 (s, 2H), 1.56 (qd,  $J = 9.2, 6.2, 4.7$  Hz, 1H), 1.30 (s, 6H), 1.24 (s, 6H), 1.07 (dd,  $J = 6.5, 1.8$  Hz, 3H), 0.90–0.82 (m, 3H). HRMS calculated for  $C_{53}H_{59}ClN_7O_7$  [ $M + H$ ]<sup>+</sup>: 940.4164, found 940.4151. UPLC retention time: 6.2 min, purity >95%.

(2*S,4R*)-*N*-((*S*)-3-(4-(((1*r,3r*)-3-(3-Chloro-4-cyanophenoxy)-2,2,4,4-tetramethylcyclobutyl)carbamoyl)phenyl)ethynyl)piperidin-1-yl)-1-(4-ethynylphenyl)-3-oxopropyl-4-hydroxy-1-((*R*)-3-methyl-2-(3-methylisoxazol-5-yl)butanoyl)pyrrolidine-2-carboxamide (21). <sup>1</sup>H NMR (400 MHz, MeOD-*d*<sub>4</sub>)  $\delta$  7.77 (dd,  $J = 19.2, 8.3$  Hz, 4H), 7.49 (dd,  $J = 17.7, 7.0$  Hz, 4H), 7.38 (d,  $J = 8.0$  Hz, 2H), 7.15 (d,  $J = 2.4$  Hz, 1H), 7.00 (dd,  $J = 8.7, 2.4$  Hz, 1H), 6.24 (d,  $J = 4.1$  Hz, 1H), 5.37 (s, 1H), 4.53–4.45 (m, 2H), 4.31 (s, 1H), 4.18 (s, 1H), 3.97–3.78 (m, 5H), 3.62 (s, 1H), 3.50 (dd,  $J = 12.5, 7.8$  Hz, 2H), 3.15–2.91 (m, 5H), 2.42 (s, 1H), 2.27 (d,  $J = 4.2$  Hz, 3H), 2.18 (d,  $J = 12.4$  Hz, 1H), 2.00 (d,  $J = 4.0$  Hz, 1H), 1.85 (s, 1H), 1.58 (s, 1H), 1.31 (s, 6H), 1.25 (s, 6H), 1.08 (d,  $J = 6.2$  Hz, 3H), 0.92–0.84 (m, 3H). HRMS calculated for  $C_{54}H_{60}ClN_6O_7$  [ $M + H$ ]<sup>+</sup>: 939.4212, found 939.4194. UPLC retention time: 6.4 min, purity >95%.

(2*S,4R*)-1-(Acetyl-L-valyl)-*N*-((*S*)-3-(4-(((1*r,3r*)-3-(3-chloro-4-cyanophenoxy)-2,2,4,4-tetramethylcyclobutyl)carbamoyl)phenyl)ethynyl)piperidin-1-yl)-3-oxo-1-phenylpropyl-4-hydroxypyrrrolidine-2-carboxamide (22). <sup>1</sup>H NMR (400 MHz, MeOD-*d*<sub>4</sub>)  $\delta$  7.79 (d,  $J = 8.1$  Hz, 2H), 7.73 (d,  $J = 8.7$  Hz, 1H), 7.49 (dd,  $J = 8.4, 2.1$  Hz, 2H), 7.36 (qd,  $J = 8.2, 1.8$  Hz, 4H), 7.26 (t,  $J = 6.9$  Hz, 1H), 7.14 (d,  $J = 2.4$  Hz, 1H), 6.99 (dd,  $J = 8.8, 2.4$  Hz, 1H), 5.39–5.29 (m, 1H), 4.56 (t,  $J = 8.2$  Hz, 1H), 4.50–4.43 (m, 2H), 4.30 (s, 1H), 4.17 (s, 1H), 3.98–3.85 (m, 2H), 3.76 (dt,  $J = 12.7, 6.4$  Hz, 2H), 3.23 (ddd,  $J = 12.7, 9.0, 3.2$  Hz, 1H), 3.02 (dq,  $J = 11.4, 8.3, 7.3$  Hz, 2H), 2.94–2.85 (m, 1H), 2.23–2.08 (m, 2H), 2.01 (d,  $J = 3.2$  Hz, 3H), 1.96 (dd,  $J = 8.7, 4.4$  Hz, 1H), 1.83 (qd,  $J = 10.8, 9.9, 4.8$  Hz, 2H), 1.55 (dtt,  $J = 18.1, 9.0, 4.4$  Hz, 2H), 1.43–1.35 (m, 1H), 1.27 (d,  $J = 23.7$  Hz, 12H), 1.04–0.96 (m, 6H). UPLC–MS calculated for  $C_{50}H_{60}ClN_6O_7$  [ $M + H$ ]<sup>+</sup>: 891.42, found 891.45. UPLC retention time: 6.0 min, purity >95%.

#### General Procedure for the Synthesis of Compound (41).

DIPEA (5 equiv) and HATU (1.2 equiv) were added to a solution of the compound 29 (1 mmol) and 38 (1.1 equiv) in DMF (2 mL). After 30 min at rt, the mixture was subjected to HPLC purification to afford compound 39 with 88% yield.

$K_2CO_3$  (1.2 equiv) and KI (0.2 equiv) were added to a solution of the intermediate 39 (0.05 mmol) and 40 (1.2 equiv) in  $CH_3CN$ . After stirring the mixture overnight at 100 °C, the solvents were evaporated under reduced pressure to afford the corresponding crude compound 41, which was purified by flash column chromatography (DCM/MeOH = 20:1) with 83% yield.

*N*-((1*r,3r*)-3-(3-Chloro-4-cyanophenoxy)-2,2,4,4-tetramethylcyclobutyl)-1-(2-hydroxyethyl)-1*H*-pyrazole-4-carboxamide (41). <sup>1</sup>H NMR (400 MHz, MeOD-*d*<sub>4</sub>)  $\delta$  8.23 (d,  $J = 0.7$  Hz, 1H), 8.02 (d,  $J = 0.7$  Hz, 1H), 7.74 (d,  $J = 8.7$  Hz, 1H), 7.14 (d,  $J = 2.4$  Hz, 1H), 7.00 (dd,  $J = 8.7, 2.4$  Hz, 1H), 4.28 (s, 2H), 4.17 (d,  $J = 1.0$  Hz, 1H), 3.93 (t,  $J = 5.2$  Hz, 2H), 3.33 (p,  $J = 1.6$  Hz, 2H), 1.30 (s, 6H), 1.22 (s, 6H). UPLC–MS calculated for  $C_{21}H_{26}ClN_4O_3$  [ $M + H$ ]<sup>+</sup>: 417.17, found 417.18. UPLC retention time: 4.4 min, purity >95%.

#### Cell Lines and Cell Culture.

All the LNCaP, VCaP, and 22Rv1 cells used were purchased from the American Type Culture Collection (ATCC). LNCaP and 22Rv1 cells were grown in RPMI 1640 (Invitrogen), and VCaP cells were grown in DMEM (Dulbecco's modified Eagle's medium) with Glutamax (Invitrogen). All of the cells were supplemented with 10% fetal bovine serum (Invitrogen) at 37 °C in a humidified 5%  $CO_2$  incubator. Cell viability was evaluated by a WST-8 assay (Dojindo) following the manufacturer's instructions. Western blotting analysis was performed as previously described.<sup>43,44</sup>

#### Quantitative Real-Time Polymerase Chain Reaction (qRT-PCR).

Real-time PCR was performed using a QuantStudio 7 Flex Real-Time PCR System as described previously.<sup>23,45</sup> RNA was purified using the Qiagen RNase-Free DNase set, and then after quantification, the extracted RNA was converted to cDNA using a High Capacity RNA-to-cDNA Kit from Applied Biosystems (Thermo Fisher Scientific). The levels of AR, TMPRSS2, FKBP5, PSA(KLK3),

and GAPDH were quantified using a TaqMan Fast Advanced Master Mix from Applied Biosystems. The level of gene expression was evaluated using a comparative CT method, which compares the CT value to GAPDH ( $\Delta CT$ ) and then to vehicle control ( $\Delta\Delta CT$ ).

**Cloning and Purification of VHL-ElonginBC Complex.** The DNA sequence of VHL (coding for residues 54–213) was constructed by PCR and inserted into a His-TEV expression vector<sup>46</sup> using ligation-independent cloning. The DNA sequences of Elongin B (encoding residues 1–118) and Elongin C (encoding residues 1–96) were constructed by PCR and inserted into pCDFDuet 1 using a Gibson assembly.<sup>47</sup> BL21(DE3) cells were transformed simultaneously with both plasmids and grown in Terrific Broth at 37 °C until an OD<sub>600</sub> of 1.2. The cells were induced overnight with 0.4 mM IPTG at 24 °C. Pelleted cells were freeze-thawed and then resuspended in 20 mM Tris-HCl (pH 7.0), 200 mM NaCl, and 0.1%  $\beta$ -mercaptoethanol (bME) containing protease inhibitors. The cell suspension was lysed by sonication, and the debris was removed via centrifugation. The supernatant was incubated at 4 °C for 1 h with Ni-NTA (Qiagen) prewashed in 20 mM Tris-HCl (pH 7.0), 200 mM NaCl, and 10 mM imidazole. The protein complex was eluted in 20 mM Tris-HCl (pH 7.0), 200 mM NaCl, and 300 mM imidazole, dialyzed into 20 mM Tris-HCl (pH 7.0), 150 mM NaCl, and 0.01% bME, and incubated with TEV protease overnight at 4 °C. The protein sample was reapplied to the Ni-NTA column to remove the His-tag. The flow through containing the VHL complex was diluted to 75 mM NaCl and applied to a HiTrap Q column (GE Healthcare). The sample was eluted with a salt gradient (0.075–1 M NaCl), concentrated, and further purified on a Superdex S75 column (GE Healthcare) pre-equilibrated with 20 mM Bis-Tris (pH 7.0), 150 mM NaCl, and 1 mM DTT. Samples were aliquoted and stored at –80 °C.

**Binding Affinities of VHL Ligands to VHL-ElonginBC Complex Protein.** The IC<sub>50</sub> and K<sub>i</sub> values of compounds were determined in competitive binding experiments. Mixtures of 5  $\mu$ L of solutions of compounds in dimethyl sulfoxide (DMSO) and 95  $\mu$ L of a preincubated protein/tracer complex solution were added into assay plates, which were incubated at room temperature for 60 min with gentle shaking. The final concentrations of VHL protein and fluorescent probe were both 5 nM. Negative controls containing the protein/probe complex only (equivalent to 0% inhibition) and positive controls containing only free probes (equivalent to 100% inhibition) were included in each assay plate. FP values in millipolarization units (mP) were measured using the Infinite M-1000 plate reader (Tecan U.S., Research Triangle Park, NC) in Microfluor 1 96-well, black, round-bottom plates (Thermo Scientific, Waltham, MA) at an excitation wavelength of 485 nm and an emission wavelength of 530 nm. IC<sub>50</sub> values were determined by nonlinear regression fitting of the competition curves. K<sub>i</sub> values of competitive inhibitors were obtained directly by nonlinear regression fitting based on the K<sub>D</sub> values of the probe and concentrations of the protein and probe in the competitive assays. All the FP competitive experiments were performed in duplicate in three independent experiments.

**Western Blotting.** Treated cells were lysed by RIPA buffer supplemented with protease and phosphatase inhibitors. The cell lysates were separated by 4–12% SDS-PAGE gels and blotted into PVDF (polyvinylidene difluoride) membranes. Software ImageJ was used to quantify the percentage of AR degradation. The net protein bands and loading controls are calculated by deducting the background from the inverted band value. The final relative quantification values are the ratio of the net band to net loading control.

## ■ ASSOCIATED CONTENT

### ● Supporting Information

The Supporting Information is available free of charge at <https://pubs.acs.org/doi/10.1021/acs.jmedchem.9b01393>.

Western blotting analysis of AR proteins in LNCaP cells treated with all AR degraders; Western blotting analysis

of ARD-266 in LNCaP, VCaP, and 22Rv1 cells; <sup>1</sup>H NMR, <sup>13</sup>C NMR, and UPLC-MS spectrum of compound ARD-266; and chemical data for VHL-a to VHL-h (PDF)

Molecular string files for all the final target compounds (CSV)

## ■ AUTHOR INFORMATION

### Corresponding Author

\*E-mail: [shaomeng@umich.edu](mailto:shaomeng@umich.edu). Phone: 1-734-615-0362.

### ORCID

Shaomeng Wang: 0000-0002-8782-6950

### Author Contributions

<sup>±</sup>X.H. and L.Z. contributed equally to this work.

### Notes

The authors declare the following competing financial interest(s): The University of Michigan has filed a patent application on these AR degraders, which has been licensed to Oncopia Therapeutics Inc. S. Wang, X. Han, C. Wang, C. Qin, W. Xiang, T. Xu, and C. Yang are co-inventors on these patents. The University of Michigan has received a research contract from Oncopia. S.W. is a co-founder of Oncopia, owns stock in Oncopia, and is a paid consultant of Oncopia.

## ■ ACKNOWLEDGMENTS

This study was supported in part by funding from Oncopia Therapeutics, LLC, and the University of Michigan Comprehensive Cancer Center Core Grant from the National Cancer Institute, NIH (grant P30CA046592).

## ■ ABBREVIATIONS

AR, androgen receptor; mCRPC, metastatic castration-resistant prostate cancer; PROTAC, proteolysis targeting chimera; ER, estrogen receptor; DC<sub>50</sub>, concentration needed to degrade 50% of AR protein; D<sub>max</sub>, maximal levels of degradation; FP, fluorescence polarization; ppm, parts per million; TMS, tetramethylsilane; MS, mass spectral; ATCC, American Type Culture Collection; qRT-PCR, quantitative real-time polymerase chain reaction

## ■ REFERENCES

- (1) Scudellari, M. Protein-slaying drugs could be the next blockbuster therapies. *Nature* **2019**, *567*, 298–300.
- (2) Lai, A. C.; Crews, C. M. Induced protein degradation: an emerging drug discovery paradigm. *Nat. Rev. Drug Discovery* **2017**, *16*, 101–114.
- (3) Sun, B.; Fiskus, W.; Qian, Y.; Rajapakshe, K.; Raina, K.; Coleman, K. G.; Crew, A. P.; Shen, A.; Saenz, D. T.; Mill, C. P.; Nowak, A. J.; Jain, N.; Zhang, L.; Wang, M.; Khoury, J. D.; Coarfa, C.; Crews, C. M.; Bhalla, K. N. BET protein proteolysis targeting chimera (PROTAC) exerts potent lethal activity against mantle cell lymphoma cells. *Leukemia* **2018**, *32*, 343–352.
- (4) Powell, C. E.; Gao, Y.; Tan, L.; Donovan, K. A.; Nowak, R. P.; Loehr, A.; Bahcall, M.; Fischer, E. S.; Jänne, P. A.; George, R. E.; Gray, N. S. Chemically induced degradation of anaplastic lymphoma kinase (ALK). *J. Med. Chem.* **2018**, *61*, 4249–4255.
- (5) Hansen, J. D.; Condroski, K.; Correa, M.; Muller, G.; Man, H. W.; Ruchelman, A.; Zhang, W.; Vocanson, F.; Crea, T.; Liu, W.; Lu, G.; Baculi, F.; LeBrun, L.; Mahmoudi, A.; Carmel, G.; Hickman, M.; Lu, C. C. Protein degradation via CRL4<sup>CRBN</sup> ubiquitin ligase: discovery and structure-activity relationships of novel glutarimide analogs that promote degradation of aiolos and/or GSPT1. *J. Med. Chem.* **2018**, *61*, 492–503.

- (6) Toure, M.; Crews, C. M. Small-molecule PROTACS: new approaches to protein degradation. *Angew. Chem., Int. Ed.* **2016**, *55*, 1966–1973.
- (7) Bondeson, D. P.; Crews, C. M. Targeted protein degradation by small molecules. *Annu. Rev. Pharmacol. Toxicol.* **2017**, *57*, 107–123.
- (8) Gustafson, J. L.; Neklesa, T. K.; Cox, C. S.; Roth, A. G.; Buckley, D. L.; Tae, H. S.; Sundberg, T. B.; Stagg, D. B.; Hines, J.; McDonnell, D. P.; Norris, J. D.; Crews, C. M. Small-molecule-mediated degradation of the androgen receptor through hydrophobic tagging. *Angew. Chem., Int. Ed.* **2015**, *54*, 9659–9662.
- (9) Testa, A.; Lucas, X.; Castro, G. V.; Chan, K. H.; Wright, J. E.; Runcie, A. C.; Gadd, M. S.; Harrison, W. T. A.; Ko, E. J.; Fletcher, D.; Ciulli, A. 3-Fluoro-4-hydroxyprolines: synthesis, conformational analysis, and stereoselective recognition by the VHL E3 ubiquitin ligase for targeted protein degradation. *J. Am. Chem. Soc.* **2018**, *140*, 9299–9313.
- (10) Gadd, M. S.; Testa, A.; Lucas, X.; Chan, K. H.; Chen, W.; Lamont, D. J.; Zengerle, M.; Ciulli, A. Structural basis of PROTAC cooperative recognition for selective protein degradation. *Nat. Chem. Biol.* **2017**, *13*, 514–521.
- (11) Zengerle, M.; Chan, K. H.; Ciulli, A. Selective small molecule induced degradation of the BET bromodomain protein BRD4. *ACS Chem. Biol.* **2015**, *10*, 1770–1777.
- (12) Churcher, I. PROTAC-induced protein degradation in drug discovery: breaking the rules or just making new ones? *J. Med. Chem.* **2018**, *61*, 444–452.
- (13) Salami, J.; Alabi, S.; Willard, R. R.; Vitale, N. J.; Wang, J.; Dong, H.; Jin, M.; McDonnell, D. P.; Crew, A. P.; Neklesa, T. K.; Crews, C. M. Androgen receptor degradation by the proteolysis-targeting chimera ARCC-4 outperforms enzalutamide in cellular models of prostate cancer drug resistance. *Commun. Biol.* **2018**, *1*, 100.
- (14) Burslem, G. M.; Crews, C. M. Small-molecule modulation of protein homeostasis. *Chem. Rev.* **2017**, *117*, 11269–11301.
- (15) Smith, B. E.; Wang, S. L.; Jaime-Figueroa, S.; Harbin, A.; Wang, J.; Hamman, B. D.; Crews, C. M. Differential PROTAC substrate specificity dictated by orientation of recruited E3 ligase. *Nat. Commun.* **2019**, *10*, 131.
- (16) Wang, P.; Zhou, J. Proteolysis Targeting Chimera (PROTAC): A Paradigm-shifting approach in small molecule drug discovery. *Curr. Top. Med. Chem.* **2018**, *18*, 1354–1356.
- (17) Zou, Y.; Ma, D.; Wang, Y. The PROTAC technology in drug development. *Cell Biochem. Funct.* **2019**, *37*, 21–30.
- (18) Pettersson, M.; Crews, C. M. Proteolysis targeting chimeras (PROTACs) - past, present and future. *Drug Discovery Today: Technol.* **2019**, *31*, 15–27.
- (19) Gu, S.; Cui, D.; Chen, X.; Xiong, X.; Zhao, Y. PROTACs: an emerging targeting technique for protein degradation in drug discovery. *BioEssays* **2018**, *40*, 1700247.
- (20) An, S.; Fu, L. Small-molecule PROTACs: An emerging and promising approach for the development of targeted therapy drugs. *EBioMedicine* **2018**, *36*, 553–562.
- (21) Zhou, B.; Hu, J.; Xu, F.; Chen, Z.; Bai, L.; Fernandez-Salas, E.; Lin, M.; Liu, L.; Yang, C. Y.; Zhao, Y.; McEachern, D.; Przybranowski, S.; Wen, B.; Sun, D.; Wang, S. Discovery of a small-molecule degrader of bromodomain and extra-terminal (BET) proteins with picomolar cellular potencies and capable of achieving tumor regression. *J. Med. Chem.* **2018**, *61*, 462–481.
- (22) Qin, C.; Hu, Y.; Zhou, B.; Fernandez-Salas, E.; Yang, C. Y.; Liu, L.; McEachern, D.; Przybranowski, S.; Wang, M.; Stuckey, J.; Meagher, J.; Bai, L.; Chen, Z.; Lin, M.; Yang, J.; Ziazadeh, D. N.; Xu, F.; Hu, J.; Xiang, W.; Huang, L.; Li, S.; Wen, B.; Sun, D.; Wang, S. Discovery of QCA570 as an exceptionally potent and efficacious proteolysis targeting chimera (PROTAC) degrader of the bromodomain and extra-terminal (BET) proteins capable of inducing complete and durable tumor regression. *J. Med. Chem.* **2018**, *61*, 6685–6704.
- (23) Bai, L.; Zhou, B.; Yang, C. Y.; Ji, J.; McEachern, D.; Przybranowski, S.; Jiang, H.; Hu, J.; Xu, F.; Zhao, Y.; Liu, L.; Fernandez-Salas, E.; Xu, J.; Dou, Y.; Wen, B.; Sun, D.; Meagher, J.; Stuckey, J.; Hayes, D. F.; Li, S.; Ellis, M. J.; Wang, S. Targeted degradation of BET proteins in triple-negative breast cancer. *Cancer Res.* **2017**, *77*, 2476–2487.
- (24) Li, Y.; Yang, J.; Aguilar, A.; McEachern, D.; Przybranowski, S.; Liu, L.; Yang, C. Y.; Wang, M.; Han, X.; Wang, S. Discovery of MD-224 as a first-in-class, highly potent, and efficacious proteolysis targeting chimera murine double minute 2 degrader capable of achieving complete and durable tumor regression. *J. Med. Chem.* **2019**, *62*, 448–466.
- (25) Hu, J.; Hu, B.; Wang, M.; Xu, F.; Miao, B.; Yang, C.-Y.; Wang, M.; Liu, Z.; Hayes, D. F.; Chinnaswamy, K.; Delproposto, J.; Stuckey, J.; Wang, S. Discovery of ERD-308 as a highly potent proteolysis targeting chimera (PROTAC) degrader of estrogen receptor (ER). *J. Med. Chem.* **2019**, *62*, 1420–1442.
- (26) Han, X.; Wang, C.; Qin, C.; Xiang, W.; Fernandez-Salas, E.; Yang, C. Y.; Wang, M.; Zhao, L.; Xu, T.; Chinnaswamy, K.; Delproposto, J.; Stuckey, J.; Wang, S. Discovery of ARD-69 as a highly potent proteolysis targeting chimera (PROTAC) degrader of androgen receptor (AR) for the treatment of prostate cancer. *J. Med. Chem.* **2019**, *62*, 941–964.
- (27) Sun, Y.; Zhao, X.; Ding, N.; Gao, H.; Wu, Y.; Yang, Y.; Zhao, M.; Hwang, J.; Song, Y.; Liu, W.; Rao, Y. PROTAC-induced BTK degradation as a novel therapy for mutated BTK C481S induced ibrutinib-resistant B-cell malignancies. *Cell Res.* **2018**, *28*, 779–781.
- (28) Saenz, D. T.; Fiskus, W.; Qian, Y.; Manshour, T.; Rajapakshe, K.; Raina, K.; Coleman, K. G.; Crew, A. P.; Shen, A.; Mill, C. P.; Sun, B.; Qiu, P.; Kadia, T. M.; Pemmaraju, N.; DiNardo, C.; Kim, M. S.; Nowak, A. J.; Coarfa, C.; Crews, C. M.; Verstovsek, S.; Bhalla, K. N. Novel BET protein proteolysis-targeting chimera exerts superior lethal activity than bromodomain inhibitor (BETi) against post-myeloproliferative neoplasm secondary (s) AML cells. *Leukemia* **2017**, *31*, 1951–1961.
- (29) Cromm, P. M.; Crews, C. M. Targeted protein degradation: from chemical biology to drug discovery. *Cell Chem. Biol.* **2017**, *24*, 1181–1190.
- (30) Cromm, P. M.; Samarasinghe, K. T. G.; Hines, J.; Crews, C. M. Addressing kinase-independent functions of fak via PROTAC-mediated degradation. *J. Am. Chem. Soc.* **2018**, *140*, 17019–17026.
- (31) Burslem, G. M.; Song, J.; Chen, X.; Hines, J.; Crews, C. M. Enhancing antiproliferative activity and selectivity of a FLT-3 inhibitor by proteolysis targeting chimera conversion. *J. Am. Chem. Soc.* **2018**, *140*, 16428–16432.
- (32) McCoull, W.; Cheung, T.; Anderson, E.; Barton, P.; Burgess, J.; Byth, K.; Cao, Q.; Castaldi, M. P.; Chen, H.; Chiarparin, E.; Carbajo, R. J.; Code, E.; Cowan, S.; Davey, P. R.; Ferguson, A. D.; Fillery, S.; Fuller, N. O.; Gao, N.; Hargreaves, D.; Howard, M. R.; Hu, J.; Kawatkar, A.; Kemmitt, P. D.; Leo, E.; Molina, D. M.; O'Connell, N.; Petteruti, P.; Rasmusson, T.; Raubo, P.; Rawlins, P. B.; Ricchiuto, P.; Robb, G. R.; Schenone, M.; Waring, M. J.; Zinda, M.; Fawell, S.; Wilson, D. M. Development of a novel B-Cell lymphoma 6 (BCL6) PROTAC to provide insight into small molecule targeting of BCL6. *ACS Chem. Biol.* **2018**, *13*, 3131–3141.
- (33) Raina, K.; Lu, J.; Qian, Y.; Altieri, M.; Gordon, D.; Rossi, A. M. K.; Wang, J.; Chen, X.; Dong, H.; Siu, K.; Winkler, J. D.; Crew, A. P.; Crews, C. M.; Coleman, K. G. PROTAC-induced BET protein degradation as a therapy for castration-resistant prostate cancer. *Proc. Natl. Acad. Sci.* **2016**, *113*, 7124–7129.
- (34) Chen, H.; Chen, F.; Pei, S.; Gou, S. Pomalidomide hybrids act as proteolysis targeting chimeras: synthesis, anticancer activity and B-Raf degradation. *Bioorg. Chem.* **2019**, *87*, 191–199.
- (35) Tinworth, C. P.; Lithgow, H.; Dittus, L.; Bassi, Z. I.; Hughes, S. E.; Muelbaier, M.; Dai, H.; Smith, I. E. D.; Kerr, W. J.; Burley, G. A.; Bantscheff, M.; Harling, J. D. PROTAC-mediated degradation of bruton's tyrosine kinase is inhibited by covalent binding. *ACS Chem. Biol.* **2019**, *14*, 342–347.
- (36) Jiang, B.; Wang, E. S.; Donovan, K. A.; Liang, Y.; Fischer, E. S.; Zhang, T.; Gray, N. S. Development of dual and selective

degraders of cyclin-dependent kinases 4 and 6. *Angew. Chem., Int. Ed.* **2019**, *63*, 6321–6326.

(37) Roy, M. J.; Winkler, S.; Hughes, S. J.; Whitworth, C.; Galant, M.; Farnaby, W.; Rumpel, K.; Ciulli, A. SPR-measured dissociation kinetics of PROTAC ternary complexes influence target degradation rate. *ACS Chem. Biol.* **2019**, *14*, 361–368.

(38) Soares, P.; Gadd, M. S.; Frost, J.; Galdeano, C.; Ellis, L.; Epemolu, O.; Rocha, S.; Read, K. D.; Ciulli, A. Group-based optimization of potent and cell-active inhibitors of the von Hippel-Lindau (VHL) E3 ubiquitin ligase: structure-activity relationships leading to the chemical probe (2*S*,4*R*)-1-((*S*)-2-(1-Cyanocyclopropanecarboxamido)-3,3-dimethylbutanoyl)-4-hydroxy-N-(4-(4-methylthiazol-5-yl)benzyl)pyrrolidine-2-carboxamide (VH298). *J. Med. Chem.* **2018**, *61*, 599–618.

(39) Buckley, D. L.; Van Molle, I.; Gareiss, P. C.; Tae, H. S.; Michel, J.; Noblin, D. J.; Jorgensen, W. L.; Ciulli, A.; Crews, C. M. Targeting the von Hippel-Lindau E3 ubiquitin ligase using small molecules to disrupt the VHL/HIF-1 $\alpha$  interaction. *J. Am. Chem. Soc.* **2012**, *134*, 4465–4468.

(40) Galdeano, C.; Gadd, M. S.; Soares, P.; Scaffidi, S.; Van Molle, I.; Birced, I.; Hewitt, S.; Dias, D. M.; Ciulli, A. Structure-guided design and optimization of small molecules targeting the protein-protein interaction between the von Hippel-Lindau (VHL) E3 ubiquitin ligase and the hypoxia inducible factor (HIF)  $\alpha$  subunit with in vitro nanomolar affinities. *J. Med. Chem.* **2014**, *57*, 8657–8663.

(41) Buckley, D. L.; Gustafson, J. L.; Van Molle, I.; Roth, A. G.; Tae, H. S.; Gareiss, P. C.; Jorgensen, W. L.; Ciulli, A.; Crews, C. M. Small-molecule inhibitors of the interaction between the E3 ligase VHL and HIF1 $\alpha$ . *Angew. Chem., Int. Ed.* **2012**, *51*, 11463–11467.

(42) Guo, C.; Linton, A.; Kephart, S.; Ornelas, M.; Pairish, M.; Gonzalez, J.; Greasley, S.; Nagata, A.; Burke, B. J.; Edwards, M.; Hosea, N.; Kang, P.; Hu, W.; Engebretsen, J.; Briere, D.; Shi, M.; Gukasyan, H.; Richardson, P.; Dack, K.; Underwood, T.; Johnson, P.; Morell, A.; Felstead, R.; Kuruma, H.; Matsimoto, H.; Zoubeidi, A.; Gleave, M.; Los, G.; Fanjul, A. N. Discovery of aryloxy tetramethylcyclobutanes as novel androgen receptor antagonists. *J. Med. Chem.* **2011**, *54*, 7693–7704.

(43) Liu, V. W. S.; Yau, W. L.; Tam, C. W.; Yao, K.-M.; Shiu, S. Y. W. Melatonin inhibits androgen receptor splice variant-7 (AR-V7)-induced nuclear factor-kappa B (NF- $\kappa$ B) activation and NF- $\kappa$ B activator-induced AR-V7 expression in prostate cancer cells: potential implications for the use of melatonin in castration-resistant prostate cancer (CRPC) therapy. *Int. J. Mol. Sci.* **2017**, *18*, 1130.

(44) Sun, H.; Nikolovska-Coleska, Z.; Lu, J.; Meagher, J. L.; Yang, C. Y.; Qiu, S.; Tomita, Y.; Ueda, Y.; Jiang, S.; Krajewski, K.; Roller, P. P.; Stuckey, J. A.; Wang, S. Design, synthesis, and characterization of a potent, nonpeptide, cell-permeable, bivalent Smac mimetic that concurrently targets both the BIR2 and BIR3 domains in XIAP. *J. Am. Chem. Soc.* **2007**, *129*, 15279–15294.

(45) Lu, J.; Bai, L.; Sun, H.; Nikolovska-Coleska, Z.; McEachern, D.; Qiu, S.; Miller, R. S.; Yi, H.; Shangary, S.; Sun, Y.; Meagher, J. L.; Stuckey, J. A.; Wang, S. SM-164: a novel, bivalent Smac mimetic that induces apoptosis and tumor regression by concurrent removal of the blockade of cIAP-1/2 and XIAP. *Cancer Res.* **2008**, *68*, 9384–9393.

(46) Stols, L.; Gu, M.; Dieckman, L.; Raffin, R.; Collart, F. R.; Donnelly, M. I. A new vector for high-throughput, ligation-independent cloning encoding a tobacco etch virus protease cleavage site. *Protein Expression Purif.* **2002**, *25*, 8–15.

(47) Benoit, R. M.; Ostermeier, C.; Geiser, M.; Li, J. S. Z.; Widmer, H.; Auer, M. Seamless insert-plasmid assembly at high efficiency and low cost. *PLoS One* **2016**, *11*, No. e0153158.